NAVAL POSTGRADUATE SCHOOL

MONTEREY, CALIFORNIA

THESIS

TETHERED OPERATION OF AUTONOMOUS AERIAL VEHICLES TO PROVIDE EXTENDED FIELD OF VIEW FOR AUTONOMOUS GROUND VEHICLES

by

Nyit Sin Phang

December 2006

Thesis Advisor:	Douglas Horner
Thesis Co-advisor:	Vladimir Dobrokhodov
Second Reader:	Anthony J. Healey

THIS PAGE INTENTIONALLY LEFT BLANK

REPORT DOCUMENTATION PAGE			Form Approved OMB No. 0704-0188
Public reporting burden for this collection of information is estimated to average 1 hour per response, including the time for reviewing instruction, searching existing data sources, gathering and maintaining the data needed, and completing and reviewing the collection of information. Send comments regarding this burden estimate or any other aspect of this collection of information, including suggestions for reducing this burden, to Washington headquarters Services, Directorate for Information Operations and Reports, 1215 Jefferson Davis Highway, Suite 1204, Arlington, VA 22202-4302, and to the Office of Management and Budget, Paperwork Reduction Project (0704-0188) Washington DC 20503.			
1. AGENCY USE ONLY *(Leave blank)*	**2. REPORT DATE** December 2006	**3. REPORT TYPE AND DATES COVERED** Master's Thesis	
4. TITLE AND SUBTITLE Tethered Operation of Autonomous Aerial Vehicles to Provide Extended Field of View for Autonomous Ground Vehicles		**5. FUNDING NUMBERS**	
6. AUTHOR(S) Nyit Sin Phang			
7. PERFORMING ORGANIZATION NAME(S) AND ADDRESS(ES) Naval Postgraduate School Monterey, CA 93943-5000		**8. PERFORMING ORGANIZATION REPORT NUMBER**	
9. SPONSORING /MONITORING AGENCY NAME(S) AND ADDRESS(ES) N/A		**10. SPONSORING/MONITORING AGENCY REPORT NUMBER**	
11. SUPPLEMENTARY NOTES The views expressed in this thesis are those of the author and do not reflect the official policy or position of the Department of Defense or the U.S. Government.			
12a. DISTRIBUTION / AVAILABILITY STATEMENT Approved for public release; distribution is unlimited		**12b. DISTRIBUTION CODE**	

13. ABSTRACT (maximum 200 words)

This thesis was part of the ongoing research conducted at the Naval Postgraduate School to achieve greater collaboration between heterogeneous autonomous vehicles. The research addresses optimal control issues in the collaboration between an Unmanned Aerial Vehicle (UAV) and Autonomous Ground Vehicles (AGV). The scenario revolves around using the camera onboard the UAV to extend the effective field of view of the AGV. For military operations, this could be helpful in improving security for convoys and riverine patrols. There were three main problems addressed in this thesis. The first problem dealt with the design of a UAV control law that takes into consideration the relative speed differences between the UAV and the AGV. The UAV was assumed to have a greater speed compared to the AGV in this thesis. The second was the keystone field of view projection effect of the UAV's onboard camera onto the earth. The image captured by the camera was distorted due to the view angle of the camera from a high elevation. The third problem addressed was control of the location of the UAV to ensure the reliability of the communication network between the UAV and the AGV. The communication was assumed to be a linear function of the relative positions of the UAV and the AGV.

14. SUBJECT TERMS Tether Control, Keystone effect, Autonomous Vehicles, Unmanned Aerial Vehicles, Unmanned Surface Vehicles.			**15. NUMBER OF PAGES** 63
			16. PRICE CODE
17. SECURITY CLASSIFICATION OF REPORT Unclassified	**18. SECURITY CLASSIFICATION OF THIS PAGE** Unclassified	**19. SECURITY CLASSIFICATION OF ABSTRACT** Unclassified	**20. LIMITATION OF ABSTRACT** UL

NSN 7540-01-280-5500 Standard Form 298 (Rev. 2-89)
Prescribed by ANSI Std. 239-18

THIS PAGE INTENTIONALLY LEFT BLANK

Approved for public release; distribution is unlimited

TETHERED OPERATION OF AUTONOMOUS AERIAL VEHICLES TO PROVIDE EXTENDED FIELD OF VIEW FOR AUTONOMOUS GROUND VEHICLES

Nyit Sin Phang
Major, Singapore Armed Forces
B. Engineering (ME), Nanyang Technological University, Singapore, 1999

Submitted in partial fulfillment of the
requirements for the degree of

MASTER OF SCIENCE IN MECHANICAL ENGINEERING

from the

NAVAL POSTGRADUATE SCHOOL
December 2006

Author: Nyit Sin Phang

Approved by: Prof. Douglas Horner
Thesis Advisor

Prof. Vladimir Dobrokhodov
Thesis Co-Advisor

Prof. Anthony J. Healey
Chairman, Department of Mechanical and Astronautical Engineering

THIS PAGE INTENTIONALLY LEFT BLANK

ABSTRACT

This thesis was part of the ongoing research conducted at the Naval Postgraduate School to achieve greater collaboration between heterogeneous autonomous vehicles. The research addresses optimal control issues in the collaboration between an Unmanned Aerial Vehicle (UAV) and Autonomous Ground Vehicles (AGV). The scenario revolves around using the camera onboard the UAV to extend the effective field of view of the AGV. For military operations, this could be helpful in improving security for convoys and riverine patrols. There were three main problems addressed in this thesis. The first problem dealt with the design of a UAV control law that takes into consideration the relative speed differences between the UAV and the AGV. The UAV was assumed to have a greater speed compared to the AGV in this thesis. The second was the keystone field of view projection effect of the UAV's onboard camera onto the earth. The image captured by the camera was distorted due to the view angle of the camera from a high elevation. The third problem addressed was control of the location of the UAV to ensure the reliability of the communication network between the UAV and the AGV. The communication was assumed to be a linear function of the relative positions of the UAV and the AGV.

THIS PAGE INTENTIONALLY LEFT BLANK

TABLE OF CONTENTS

THIS PAGE INTENTIONALLY LEFT BLANK

LIST OF FIGURES

THIS PAGE INTENTIONALLY LEFT BLANK

ACKNOWLEDGMENTS

I would like to acknowledge and express my gratitude for the support and guidance given by Prof. Douglas Horner during the course of this research. Special thanks to Prof. Vladimir Dobrokhodov for providing the Matlab model for his work [7] on "Vision-Based Tracking and Motion Estimation for Moving Targets using Small UAVs" as a reference for the development of the simulation for this thesis. Thanks to my wife, Natalie Chee, for her support and understanding during the period of research and for taking care of the children.

THIS PAGE INTENTIONALLY LEFT BLANK

I. INTRODUCTION

The rapid advancement of computer and sensor technology in recent years has resulted in an increased number of unmanned vehicles being employed in the battlefield to accomplish various dangerous tasks; one such application is the employment of unmanned vehicles for the detection and avoidance of mines and Improvised Explosive Devices (IED). The employment of unmanned vehicles for the above mentioned task usually has little interaction with other unmanned vehicles.

The current trend of employing unmanned vehicles in the battlefield has extended beyond a single vehicle operation and is moving towards the gathering of real-time information using multiple unmanned vehicles. This could potentially impact a wide variety of military missions. The employment of multiple types of unmanned vehicles is a challenge for developers for a number of reasons. First, there is the communication necessary between the vehicles. Since the vehicles are generally small, the communication equipment carried on the unmanned vehicles is usually size- and power-limited therefore resulting in corresponding limitations in bandwidth and range. Second, new guidance controls are necessary for developing collaborative behaviors between unmanned platforms. Third, there are always logistic and maintenance issues associated with using an unmanned vehicle and this is multiplied by the number of vehicles used.

The control of a single unmanned vehicle has been explored intensively and much success has been achieved. These successes have been demonstrated in the obstacle avoidance and re-routing capabilities of unmanned vehicles like Micromouse [1], a competition that started in the late 1970s, with small robot mice solving a 16 x 16 maze autonomously. Seydou SOUMARE in [2] has discussed, in depth, the uses of active vision sensors and laser sensors for real-time obstacle detection and avoidance in an indoor environment. Juan Carlos Rosete Fonseca in [3] has discussed the use of obstacle avoidance in the path planning of polar robots that allows the unmanned polar robots to perform path planning for greater autonomy and robustness. These discussions were based on indoor or laboratory environment studies that are not suitable for employment in the harsh environment of military operations.

Matthew Spenko in [4] proposed the concept of using trajectory space for high speed hazard avoidance in rough terrain. The concept proposed uses a compact framework for analyzing an unmanned ground vehicle's (UGV's) dynamic performance on uneven, natural terrain. The trajectory space defines the UGV's performance limits based on vehicle parameters, terrain features, and hazard (obstacle) properties that are applicable to military operations. However, these are limited to single vehicle operations.

The obstacle avoidance and path planning technology has extended beyond the UGV to UAVs as presented by Stephen Griffiths in [5]. These articles presented the ability to incorporate obstacle and terrain avoidance into real-time path planning by miniature aerial vehicles (MAVs), while taking into consideration the limitation of the MAV, which requires moving at a speed of 10 - 20 m/s to maintain flight. The limited payload of a MAV, as addressed in the articles, restricts the size of the onboard computer and the sensors that are employed to effectively survey the environment.

Much work has also been done in the area of obstacle avoidance and path planning by an underwater vehicle as discussed by Yvan Petillot in [6]. These articles proposed a framework for the segmentation of sonar images, tracking of underwater objects, and motion estimations for obstacle avoidance and path planning by an underwater vehicle. Douglas P. Horner in [7] has also successfully demonstrated the ability to conduct underwater surveys and the avoidance of uncharted obstacles using Autonomous Underwater Vehicles (AUVs). The above discussions have been centered on individual platforms and do not address the problem of integrating the various platforms for an integrated mission. However, with the maturity of autonomous technology on each individual platform, there is an impetus for further research in the area of collaborative operations of various platforms to perform a specific mission.

This thesis looks into the problems of developing a new guidance control law for a UAV to operate collaboratively with an AGV. The purpose of integrating a UAV with an AGV is to enhance the effectiveness of the AGV by providing an extended field of view through the UAV. The UAV, with its high maneuverability and altitude, is able to provide the advantage of forward reconnaissance for the ground vehicles. Another

advantage of using the UAV is the ability to provide a better look-ahead stand-off position and thus enable the ground vehicle to minimize contact with potential ground threats.

In this scenario, the AGV is used as a forward ground reconnaissance vehicle. Its purpose is to identify potential threats to the trailing convoy. The ability to integrate the UAV and the AGV effectively will mean that the AGV would be able to tap into the advantage of stand-off reconnaissance by the UAV, thus allowing the AGV to have a fast response to any obstacles and a longer time to effectively change its planned mission or path. The stand-off reconnaissance ability would provide advance warning to ground vehicles on ambushes within its path, and thus increase the survivability of the ground vehicle and allow better force preservation.

For the vehicles to work collaboratively, the UAV guidance law must compensate for the maneuvering AGV. Vladimir N. Dobrokhodov, in [8], has discussed extensively the influence of the AGV ground speed on the performance of the UAV following the flight path generated. The proposed concept of a circular flight path for the UAV could be adapted for the integration of a UAV and an AGV, which would allow for speed compatibility/adjustment of the fast-flying UAV with the slower-moving AGV. This concept will be used in the construction of the simulation in this thesis.

Another problem associated with integration of the UAV and the AGV is the ability to synchronize its routes and path planning algorithm to allow better autonomy of the vehicles, such that the UAV and the AGV could operate independently when communication between the vehicles is disrupted. This would allow the UAV to predict the location of the AGV based on the mission profile. The synchronization of routes and path planning algorithm will not be discussed in this thesis.

The development of computer vision algorithm for object detection and tracking enables the autonomous vehicles to detect obstacles and to track a target. This would greatly improve the autonomy of the autonomous vehicles and allows for minimum operator interference. The computer vision for autonomous vehicles will not be addressed in this thesis.

Communication and collaboration between the UAV and the AGV is of paramount importance to the success of a forward ground reconnaissance for a trailing convoy mission. The limited payload allowed on the UAV poses as a problem to incorporate a larger and higher power transmitter for long range communication. Thus the communication range between the vehicles is limited by the capability of the communication equipment that is carried by the UAV. This was highlighted by Stephen Griffiths in [5]. One solution that is proposed by Douglas P. Horner [9] is the use of an artificial potential field for UAV guidance and optimization of WLAN communication, which would optimize the communication between the UAV and a series of AGVs using the signal strength ratio. Another method discussed in this report is in using the received signal strength to form a linked control to limit the extended range of the UAV; such control mechanisms are referred to as "tether control" in this thesis.

The tether control uses the received signal strength between the UAV and the AGV to effectively control the flight path of the UAV and ensure reliable communication between the two vehicles. The method employed essentially makes use of the received signal strength to form an artificial dome around the AGV to demarcate the limits of reliable communication. If the UAV flies beyond the dome, communication is assumed to be disrupted, thus the artificial dome contains the furthest flight path of the UAV to be within this field.

The effectiveness of the UAV greatly depends on its ability to keep the onboard camera pointing at a fixed distance forward of the AGV. The camera system available on the UAV in the study has a zoom control and a two-degree-of-freedom (DOF) motion, namely, pan and tilt. The UAV in flight has a six-DOF and it is essential that the camera is able to operate in such a manner that it complements the state condition of the UAV to effectively point the camera at a fixed position forward of the AGV. Vladimir N. Dobrokhodov in [8] has discussed the use of vision-based tracking and motion estimation for moving targets using small UAVs. The concept proposed integrates UAV gimbal control with guidance of the UAV that allows tracking of a moving coordinate ground vehicles. This concept requires several geometrical transformation mathematical

computation, which is within the capability of the computer onboard the UAV. This thesis will adapt the algorithm discussed for the implementation flight control of the UAV.

The pin-hole camera model was used for this thesis, where the image captured is projected onto the earth's surface. A working assumption for the thesis is that the surface of the earth is considered to be a plane and three-dimensional earth surface model is recommended for future work. At high elevation and tilt angles, a larger area will be captured at the far-field and a smaller area at the near-field. Such effect is commonly known as the keystone effect of the camera, which is discussed by Andrew Woods in [10]. The ability to accurately demark the keystone effect will allow the image processing unit to interpret the captured image as illustrated in Figure 1. The model provides a basis for the image processing unit to correct the error and thus improve the accuracy of the data.

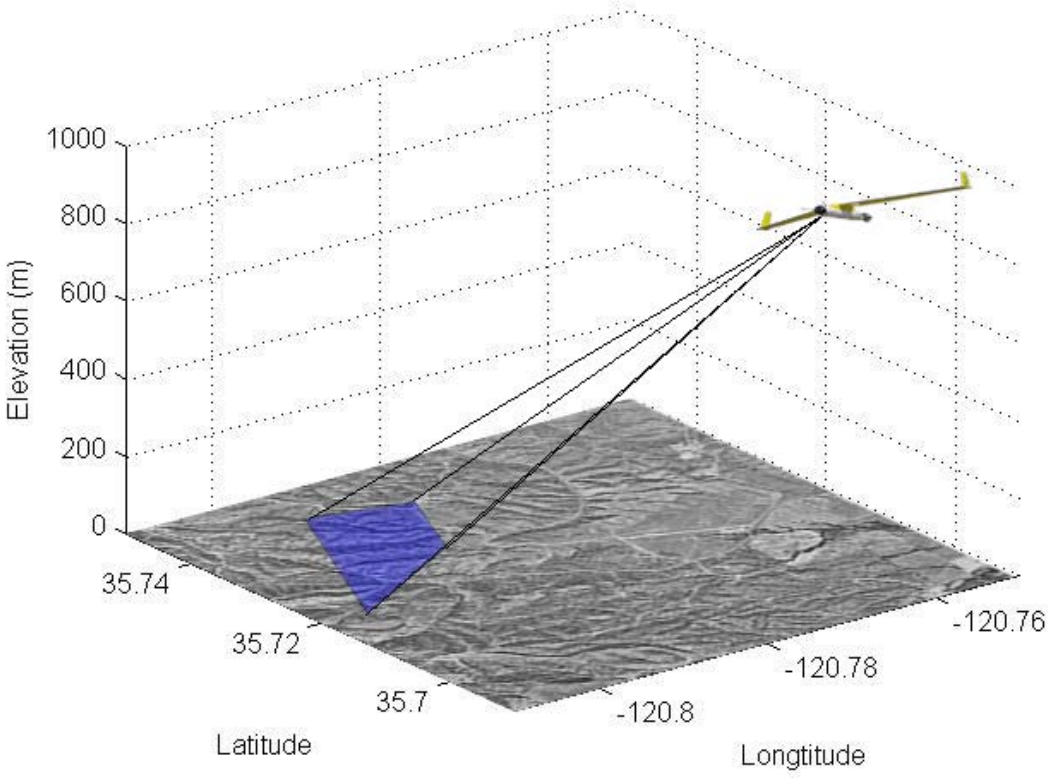

Figure 1. Keystone Effect of the Camera

This thesis was set forth to research the problem associated with integrating the existing UAV (Scan Eagle) with an AGV to provide real-time communication between the vehicles in a truly cooperative environment in order for the vehicles to achieve their mission. The model uses Matlab Simulink Version 6.4 (R2006a) [11] to simulate the UAV flying in six-DOF and incorporate the onboard camera to point at a fixed distance forward of the AGV. The AGV in the simulation has two-DOF and is programmed to travel on a road using a GeoTiff Map [12 and 13].

This thesis uses the operational concept of an AGV traveling along a road and a UAV is tethered to the AGV to provide reconnaissance images of a fixed distance forward of the AGV as shown in Figure 2.

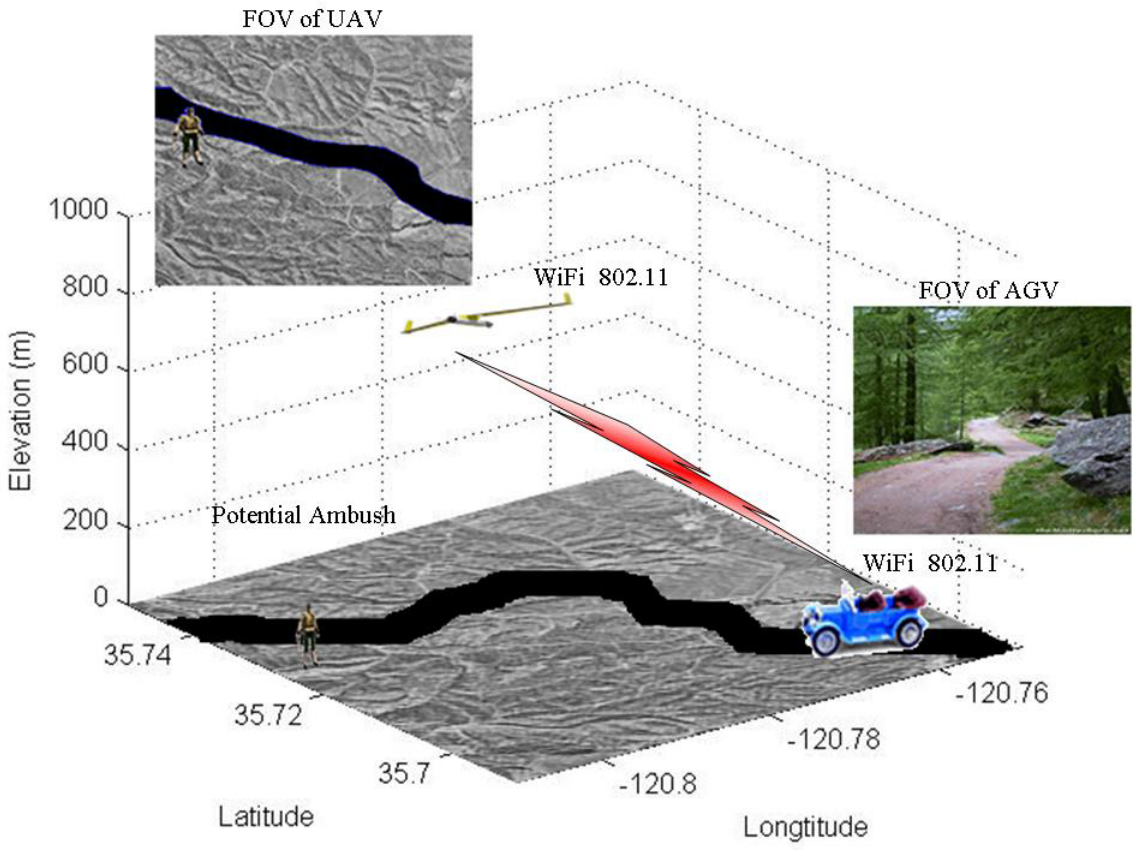

Figure 2. Operational Concept

The vehicles are equipped with standard WiFi 802.11 communication equipment (ITT Mesh Card) that has a limited range of communication. The assumption made in for

this thesis is that the signal-to-noise ratio (SRN) of the communication equipment is a linear function of distance. The figure above shows the field of view (FOV) of both vehicles. The AGV has a limited FOV due to the obstruction from the natural feature on the ground, however, the UAV, due to its operating altitude, is able to acquire a better FOV and identify a possible ambush site. The UAV images are transmitted to the AGV for further analysis. As a result of the analysis, the AGV can change its planned path or prepare for a counter attack.

The UAV used for discussion in this thesis is the newly acquired NPS Scan Eagle developed by Boeing. It weighs 18 kg and is designed for a continuous mission of more than 15 hours, with a cruising speed of 50 knots, and at maximum altitude of 5,000 meters. Scan Eagle has a carrying capacity of 6 kg and can be launched and retrieved over any terrain including onboard a ship during naval operations. The UAV system includes a Sky Wedge hydraulic launcher, Sky Hook retrieving system, and a mobile ground control element as shown below.

Figure 3. NPS Scan Eagle

Figure 4. Scan Eagle Launching System

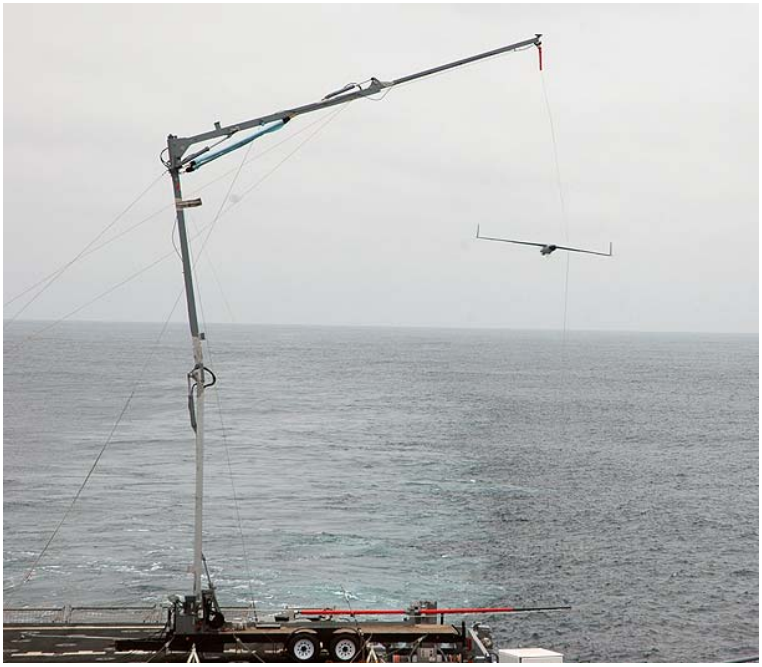

Figure 5. Scan Eagle Recovery System

Scan Eagle was designed with a removable avionics bay and two expansion slots allowing seamless payload integration. Its vision system incorporates a Sony FCB-EX780S camera with two-axis stabilization. The camera line-of-sight is gyro-stabilized with a 5-hertz bandwidth, and further electronically stabilized by Sony's SteadyShot™ with a 3 to 20 hertz bandwidth. The camera has a continuous pan capability utilizing slip-rings and a tilt angle of positive 30 degrees to negative 110 degrees. The camera has a 25:1 optical zoom from 45 degrees to 1.8 degrees FOV and a 12:1 digital zoom from 1.8 degrees to 0.15 degrees. The camera is able to operate in stabilized line-of-sight (LOS), waypoint tracking, or target tracking modes.

THIS PAGE INTENTIONALLY LEFT BLANK

II. THEORETICAL APPROACH TO MODELING THE TETHER OPERATION OF THE UAV AND AGV

A. OVERVIEW OF THE MODEL

The approached taken for this thesis is based on modeling using Simulink Version 6.4 (R2006a) as shown in Figure 6. The model is divided into five components, namely, the six-DOF model for the UAV, the camera gimbal control model, the camera keystone model, the UAV flight path control model, and the tether control model. The model is adapted from the work done in [8].

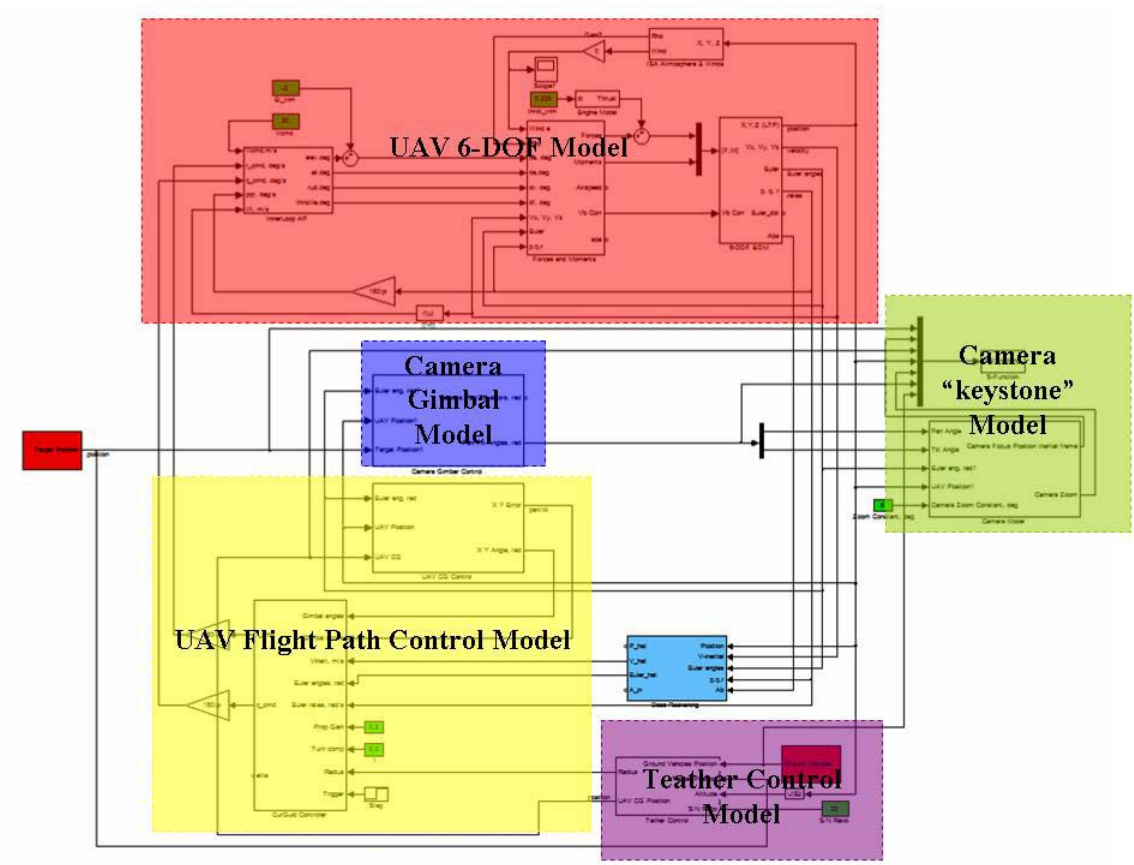

Figure 6. Overview of Model [After: 8]

B. UAV SIX-DOF FLIGHT MODEL

The UAV six-DOF model served as a basis for the simulation as it provides the required state condition of the UAV for the model to operate. Brian L. Stevens in [14]

discussed in detail the methodology for modeling the state condition for an aircraft, which is applicable to the modeling of the UAV. Figure 7 shows the UAV six-DOF model for the simulation. The model is comprised of three components, namely, the Autopilot, Forces and Moments, and the Six-DOF equations of motion model.

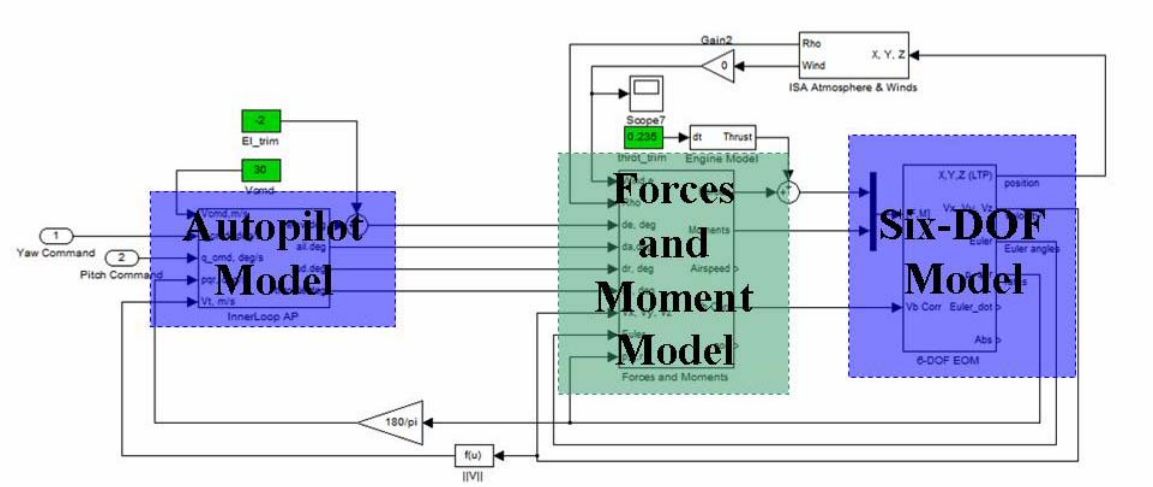

Figure 7. UAV Six-DOF Model

The autopilot model generates the required elevator, aileron, rudder deflection and throttle control using the state condition (roll, pitch, yaw, position, and velocity) of the UAV based on the yaw, pitch command input. The autopilot consists of several control loops providing stabilization of attitude, altitude and the speed of the UAV.

The Forces and Moments model receives inputs from the outputs of the autopilot and couples it with the state condition of the UAV to generate the forces and moments acting on the UAV. The forces and moments model essentially takes the elevator, aileron and rudder deflection, and based on the state condition, resolves the forces into three components, namely, the X (F_X), Y (F_Y) and Z (F_Z) components, with respect to the body frame coordinates of the UAV as shown in Figure 8. It calculates the moments generated by these forces on the three principal body axes of the UAV, as shown.

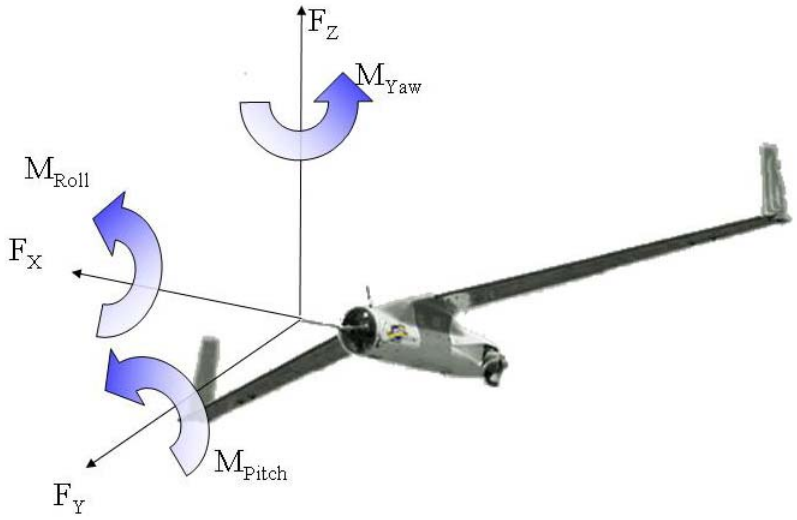

Figure 8. Forces and Moment on a UAV

The moments (T_B) generated by the inertial and combination of forces and motion of the UAV in the airframe-body coordinate (ABC) are calculated based on the following equations:

$$T_B = \dot{H}_B + \omega_B \times H_B \tag{1}$$

where H_B is the angular momentum vector, ω_B is the absolute angular velocity vector in ABC as follows:

$$\omega_B = \begin{bmatrix} P \\ Q \\ R \end{bmatrix} = \begin{bmatrix} \dot{\phi} - \dot{\psi}\sin\theta \\ \dot{\theta}\cos\phi + \dot{\psi}\cos\theta\sin\phi \\ \dot{\psi}\cos\theta\cos\phi - \dot{\theta}\sin\phi \end{bmatrix} \tag{2}$$

$$H_B = \begin{bmatrix} PJ_x & -QJ_{xy} & -RJ_{xz} \\ QJ_y & -RJ_{yz} & -PJ_{xy} \\ RJ_z & -PJ_{xz} & -QJ_{yz} \end{bmatrix} \tag{3}$$

The angular velocity vector is a composite of P (roll rate), Q (pitch rate) and R (yaw rate) of the UAV. The ϕ (roll), θ (pitch), ψ (yaw), are the Euler angles and $\dot{\phi}$, $\dot{\theta}$ and $\dot{\psi}$ are the rate of change of the Euler angles. J is the 3x3 tensor of inertia of the UAV, comprising 9 individual components.

The Six-DOF equations of motion model uses the forces and moments inputs, coupled with the current state condition of the UAV to compute the next state condition. The simulation uses a flat earth model (North-East-Down, NED), which is sufficiently accurate for the current application. The flat earth model ignores the earth's rotation (ω_E) terms and uses the Navigation Equation (4), Force Equation (5) and Moment Equation (6) to compute the states:

$$\dot{p} = B^T V_B \tag{4}$$

$$\dot{V}_B = \tfrac{1}{m} F_B - \omega_B \times V_B \tag{5}$$

$$\dot{\omega}_B = -J^{-1}\left(\omega_B \times \left(J\omega_B\right)\right) + J^{-1}T_B \tag{6}$$

The navigation equation provides the derivative of the position in the NED coordinate, where B is the transformation matrix for ABC to the NED coordinate and V_B is the absolute velocity of the UAV in ABC. The forces equation gives the derivative of velocity in ABC, where F_B is the applied forces in ABC. The moment equation gives the derivative of the absolute angular velocity vector in ABC, where J is the inertia matrix as follows:

$$J = \begin{bmatrix} J_x & -J_{xy} & -J_{xz} \\ J_y & -J_{yz} & -J_{xy} \\ J_z & -J_{xz} & -J_{yz} \end{bmatrix} \tag{7}$$

Integrating the derivative of the position, velocity, and absolute angular velocity vector will provide the absolute position in the NED coordinate, velocity and absolute angular velocity vector in ABC of the UAV. These would be used for the simulation.

C. UAV FLIGHT PATH CONTROL ALGORITHM

The UAV in flight is assumed to travel at a higher speed compared to the AGV and it is crucial to control the flight path in accordance with the average speed of the AGV. The flight path control algorithm achieved this by commanding the UAV to fly in a circular motion with respect to an imaginary moving target called the UAV CG. The

UAV CG is controlled by the tether control algorithm to achieve a constant communication link between the UAV and the AGV. The flight path of the UAV is illustrated in Figure 9 below with a moving UAV CG.

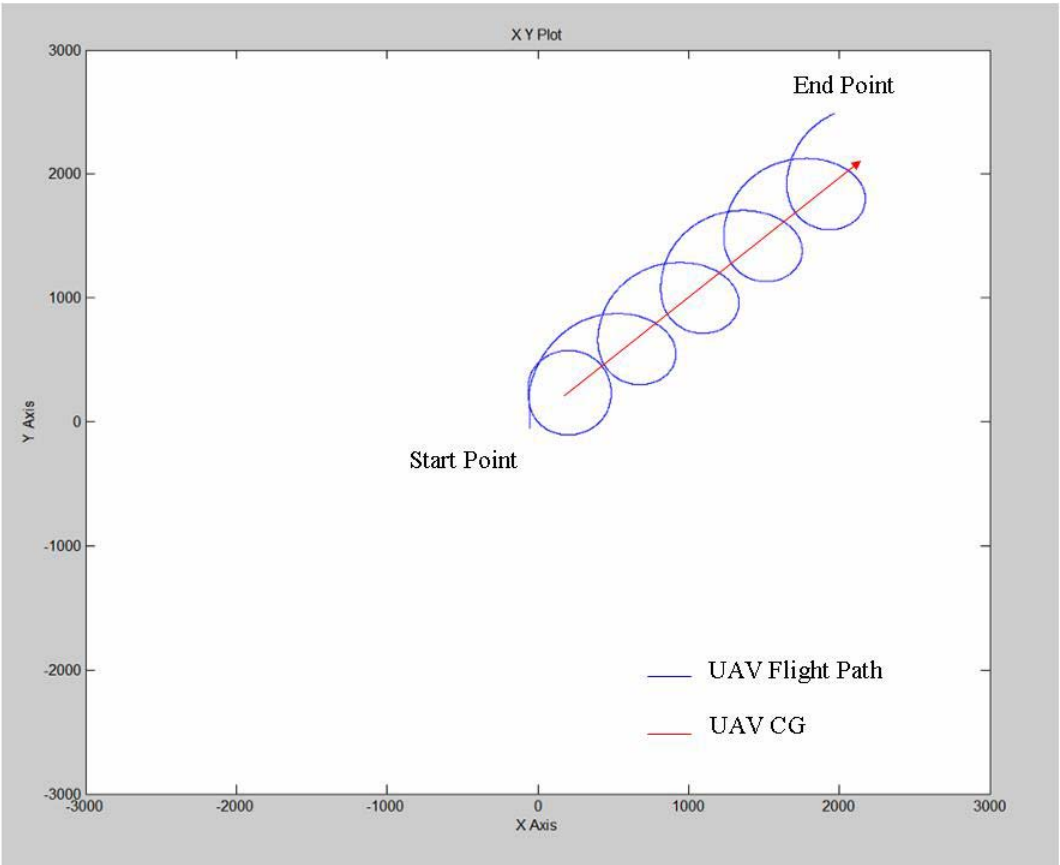

Figure 9. Flight Path of UAV with Moving UAV CG

The UAV flight path control algorithm adapted the control algorithm proposed in [7] and is shown in Figure 10.

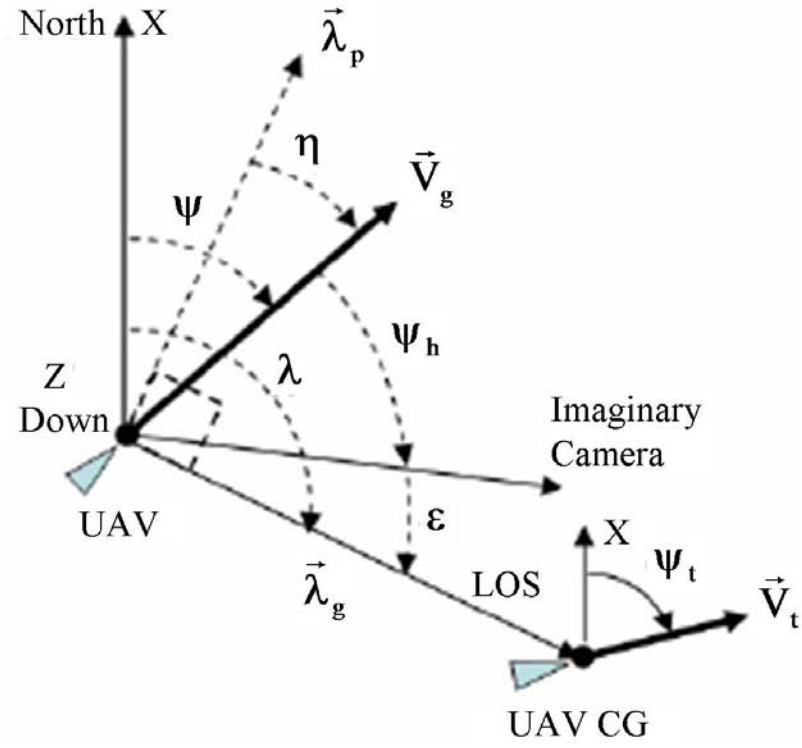

Figure 10. UAV Tracking of Imaginary Moving Target [From: 6]

From Figure 10, $\vec{V}_g$ is the UAV ground speed, $\vec{\lambda}_g$ is the line of sight (LOS) vector, $\vec{\lambda}_p$ is the vector perpendicular to $\vec{\lambda}_g$, ε is the angle between the LOS vector and the camera heading, λ is the LOS angle, ψ is the UAV heading, ψ_h is the gimbal pan angle , η is the angle between the $\vec{V}_g$ and $\vec{\lambda}_p$ vectors, $\vec{V}_t$ is the speed of the imaginary target and ψ_t is the heading of the imaginary target. The tracking problem kinematics for the target are given by:

$$\dot{\eta} = -\frac{V_g \cos\eta - V_t \cos\left(\psi_t - (\psi - \eta)\right)}{\rho} + \dot{\psi} \tag{8}$$

$$\dot{\varepsilon} = \frac{V_g \cos\eta - V_t \cos\left(\psi_t - (\psi - \eta)\right)}{\rho} - \dot{\psi} - \dot{\psi}_h \tag{9}$$

$$\dot{\rho} = -V_g \sin\eta + V_t \cos\left(\psi_t - (\psi - \eta)\right) \tag{10}$$

ρ is the range from the UAV to the imaginary target. The objective of the control system is to drive ε and η to zero using the UAV turn rate $\dot{\psi}$ and pan rate $\dot{\psi}_h$ as control inputs, thus the control law is as follows:

$$\dot{\psi} = \frac{V_g}{\rho_h}\cos\eta - k_1\eta \tag{11}$$

$$\dot{\psi}_h = k_1\eta + k_2\varepsilon \tag{12}$$

where ρ_h is the desired horizontal range to the target as user-adjustable input variables and, k_1 and k_2 are gains for the control.

The UAV flight path control model results in the UAV flying in a circular path with respect to an imaginary reference point on the ground (UAV CG). The camera vector shown in Figure 10 is an imaginary camera and does not represent the actual onboard camera of the UAV. However it is used for the control law development. The coordinated (camera and UAV guidance) control law eliminates the need for the AGV to constantly control the flight path of the UAV and reduce the computation burden of the AGV. It also allows the UAV greater flexibility to modify its flight path to avoid obstacles or adjust its height to avoid detection. The control law also allows greater autonomy to the UAV and thus forms the backbone for the successful implementation of the tether control. The onboard camera is controlled by a separate control algorithm called the camera gimbal control algorithm.

D. CAMERA GIMBAL CONTROL ALGORITHM

The camera gimbal control algorithm allows the camera to operate independently from the flight path of the UAV. The camera is programmed to point on the road a fixed distance in front of the AGV. This is achieved by giving a position coordinate called the "target" to the camera gimbal control model as illustrated in Figure 11. The camera is initially set to zero degree pan and tilt. When a target coordinate is received, the camera gimbal control model will compute the required pan and tilt angle for the camera gimbal servo mechanism to position the camera. Refer to Appendix A for the camera gimbal control model.

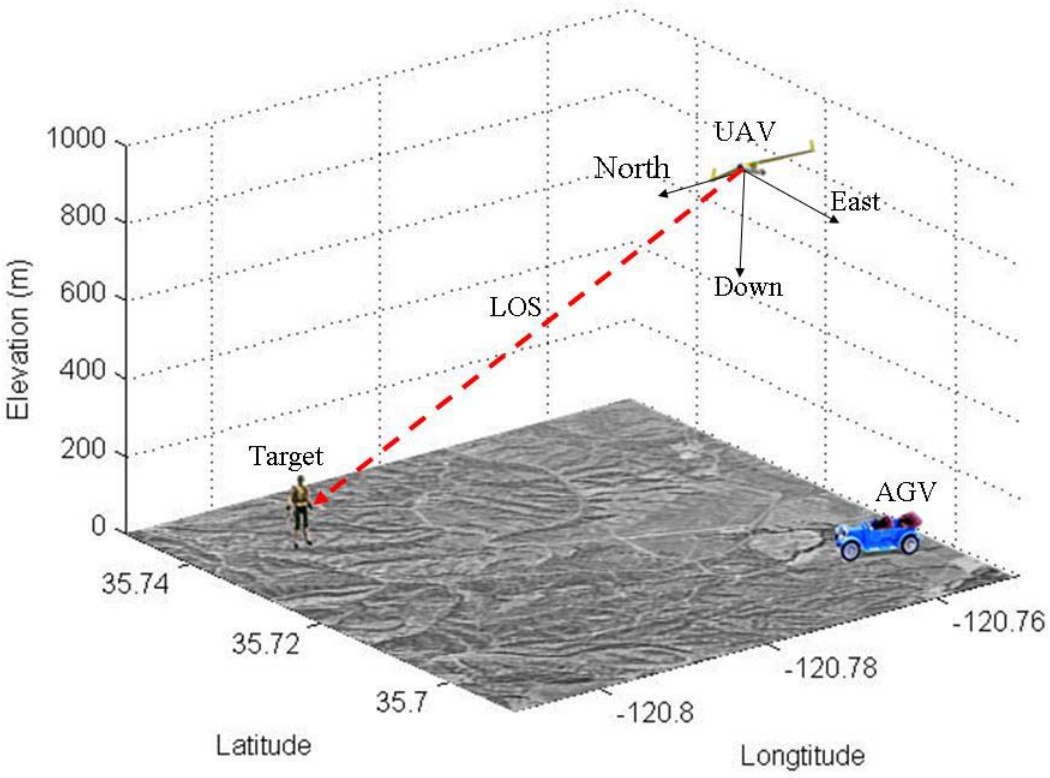

Figure 11. Camera Tracking of Ground Target

From Figure 11, Δ_x, Δ_y and Δ_z were defined as the relative position of the UAV and the ground target in ABC, ϕ_p and ϕ_t is the desired pan and tilt angle of the camera. The objective of the control law is to provide the pan and tilt error, ε_p and ε_t, to a proportional and integral controller, which in turn, commands the camera to adjust its position as follows:

$$\phi_p = \tan^{-1}\left(\frac{\Delta_y}{\Delta_x}\right)_{ABC} \tag{13}$$

$$\phi_t = \tan^{-1}\left(\frac{\Delta_z}{\sqrt{\Delta_x^2 + \Delta_y^2}}\right)_{ABC} \tag{14}$$

$$\varepsilon_p = \phi_p - \phi_{cp} \tag{15}$$

$$\varepsilon_t = \phi_t - \phi_{ct} \tag{16}$$

The control algorithm uses the relative position of the UAV and ground target in the NED coordinate and translate them to ABC using the following formula:

$$\begin{bmatrix} \Delta_x \\ \Delta_y \\ \Delta_z \end{bmatrix}_{ABC} = B \begin{bmatrix} X_t - X_u \\ Y_t - Y_u \\ Z_t - Z_u \end{bmatrix} \tag{17}$$

X_t, Y_t and Z_t is the position of the ground target, X_u, Y_u and Z_u is the position of the UAV in the NED coordinate and B is the Direct Cosine Matrix for transformation from the NED coordinate to ABC as follows:

$$B = \begin{bmatrix} \cos\theta\cos\psi & \cos\theta\sin\psi & -\sin\theta \\ \sin\phi\sin\theta\cos\psi - \cos\phi\sin\psi & \sin\phi\sin\theta\sin\psi + \cos\phi\cos\psi & \sin\phi\cos\theta \\ \cos\phi\sin\theta\cos\psi + \sin\phi\sin\psi & \cos\phi\sin\theta\cos\psi - \sin\phi\cos\psi & \cos\phi\cos\theta \end{bmatrix} \tag{18}$$

This control allows the camera to track an independent ground target, taking into consideration the state position of the UAV, thus decoupling the flight control of the UAV from the camera.

E. CAMERA KEYSTONE MODEL

Due to the position and focusing of the camera on the target at an elevated angle, the captured image will be distorted because of the keystone effect. Understanding the keystone effect will allow the image processing of the captured picture to be more accurate. The model that simulates the keystone effect is illustrated in Figure 12. Refer to Appendix B for the camera keystone model.

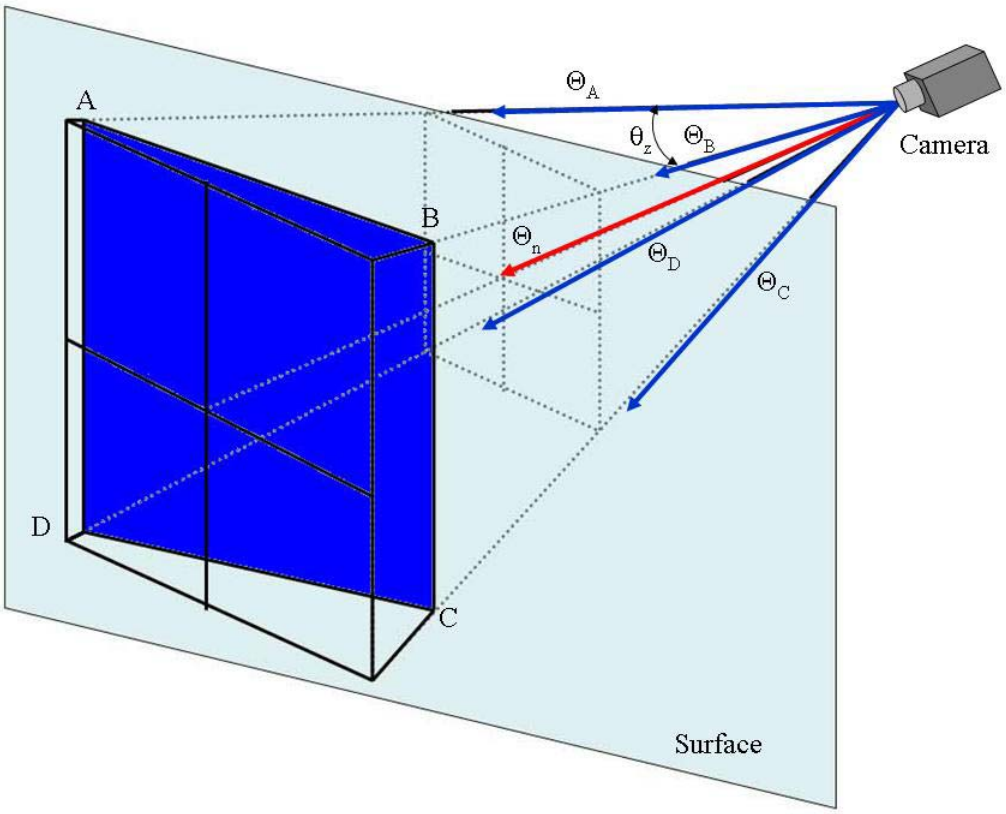

Figure 12. Modeling the Camera Keystone Effect

Θ_n is the unit vector of the camera. Using the zoom angle of the camera (θ_z), four unit vectors (Θ_A, Θ_B, Θ_C and Θ_D) could be derived to point at the four corners, A, B, C and D as shown in Figure 12. The point interceptions of the four unit vectors with the surface will give the coordinates of A, B, C and D. The dark shaded region is the area captured by the camera image.

The assumption of a pin-hole camera is used for the camera keystone model where the image captured is assumed to be proportional to the image that the camera sees as illustrated in Figure 13 below. The light from the actual object passes through the pin-hole and is projected on the back of the box as the image is captured. The distortion on the captured image, due to the lens of the camera, is not taken into consideration for the simulation.

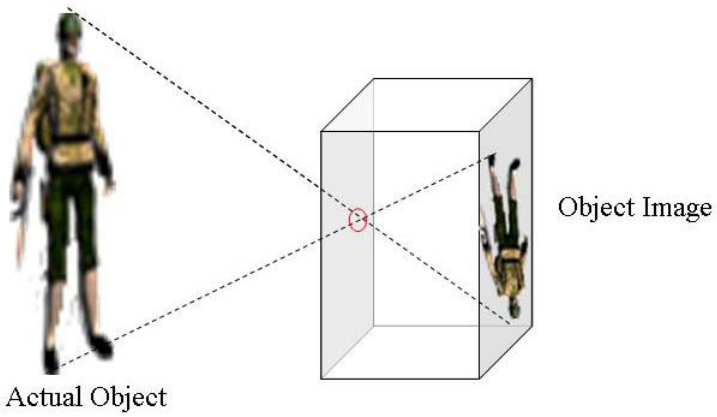

Figure 13. Pin-hole Camera Assumption

F. TETHER CONTROL FOR EFFECTIVE COMMUNICATION

The tether control model creates an invisible tether link between the UAV and the AGV to ensure that the UAV is flying at a predictable distance away from the AGV. This distance is determined by the received signal strength of the communication equipment on the UAV and the AGV. The communication equipment used on both vehicles for the exchange of information is WiFi 802.11, the wireless communication bandwidth. It is assumed that each vehicle has the capability to monitor the strength of the received signal, and using the received signal strength from the AGV, the UAV is able to adjust the distance to the AGV to ensure and maintain good communication. The SNR measurement of the radio signal from the UAV is loosely defined as an "invisible tether" since it is the SNR that determines the maximum distance the UAV can fly from the AGV.

The tether control model uses the received signal strength and the UAV LOS to the AGV to determine the distance of the invisible tether and the desired horizontal range, ρ_h.

$$\rho_h = kZ_u \tag{19}$$

The k value depends on the flight characteristics of the UAV and is selected via trial and error. The desired horizontal range increases proportionally with the altitude of the UAV to ensure the stability of the UAV flight path control law. The tether control concept is illustrated in Figure 14. It should be noted that the received signal strength

used in this model is an operator input and is the mean of the received signal strength. The actual received signal strength might fluctuate constantly due to the presence of noise in the signal, and special care has to be taken to filter the unwanted noise. Refer to Appendix C for the simulation model.

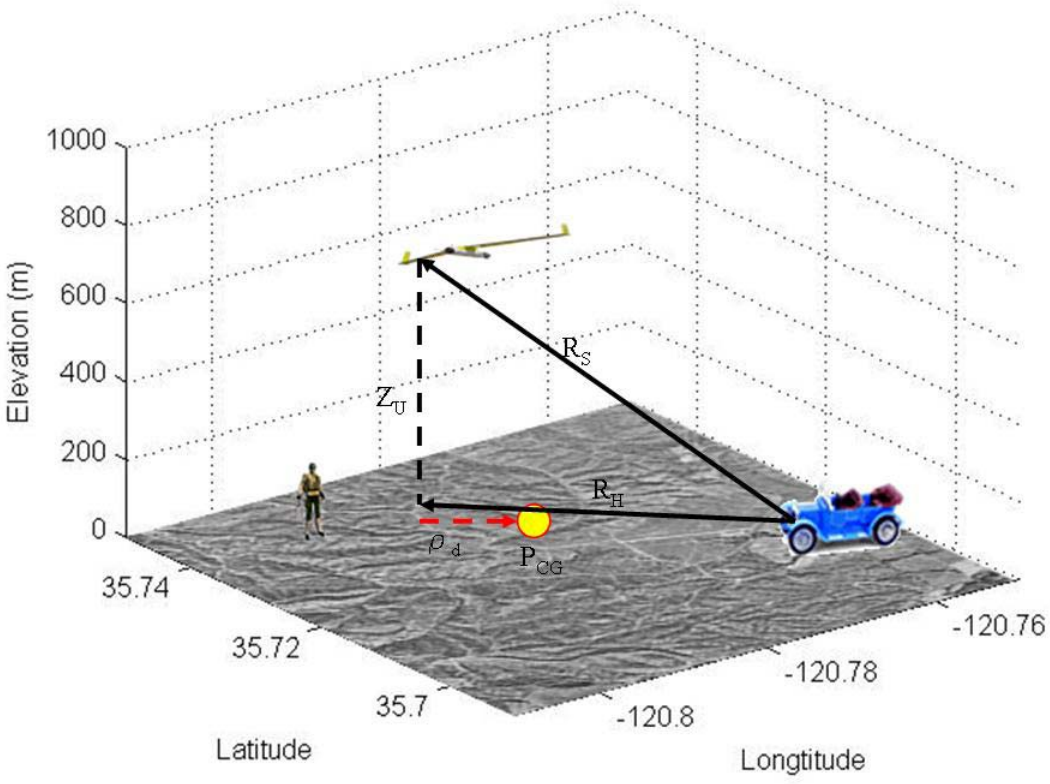

Figure 14. Tether Control between UAV and AGV

From Figure 14, R_S is the maximum communication range to ensure reliable communication, S_N is the received signal strength from the onboard communication equipment, and R_H is the horizontal vector of R_S. For this thesis, an operator input value for S_N is used for the simulation and R_S is determined by the equation below:

$$R_s = k_c S_N \tag{20}$$

k_c is the proportional gain which should be set by the operator for optimum value of R_S, which has the longest possible distance with reliable communication. The tether control uses the altitude of the UAV to determine the optimum ρ_h using a gain controller as follows:

$$P_{CG} = \begin{pmatrix} X_g \\ Y_g \\ Z_g \end{pmatrix} + \left(R_H - \rho_h \right) \tag{21}$$

where P_{CG} is the UAV CG position and X_g, Y_g and Z_g is the position of the AGV in the NED. For the tether control to be effective, the selection of the k value is important to ensure that the UAV flight path is stable

G. INTEGRATING THE MODEL

The UAV six-DOF flight model acts as the backbone for the simulation. It provides the state conditions of the UAV that are used by the rest of the model. The AGV and the desired fixed distance forward of the AGV are designed to travel on a road represented by a series of discreet coordinates along the route with one meter spacing. These coordinates are based on a relative position referenced to a fixed point on the GeoTiff maps. The speed and starting location of the AGV and the forward fixed position are controlled by the user in the model.

The tether control model uses the position of the UAV and the AGV, the received signal strength, and the UAV altitude to compute both the UAV CG location and the desired horizontal range for the UAV. The UAV CG location and the desired horizontal range are passed into the UAV flight path control model to generate the desired flight path for the UAV. The UAV flight path model outputs the pitch and yaw command for the UAV six-DOF model to compute the state condition of the UAV.

The flight path of the UAV, with respect to a moving UAV CG location, is shown previously in Figure 9. It shows that the UAV is traveling in a circular path to compensate for the slower speed AGV. An alternative, commanding the UAV to adopt an "S" curve flight path to compensate for the slower speed AGV, has been explored and is illustrated in Figure 15. Such a flight path was deemed ineffective and undesirable as the error generated for the camera during the turn is large and caused the camera to momentarily lose its focus on the desired location.

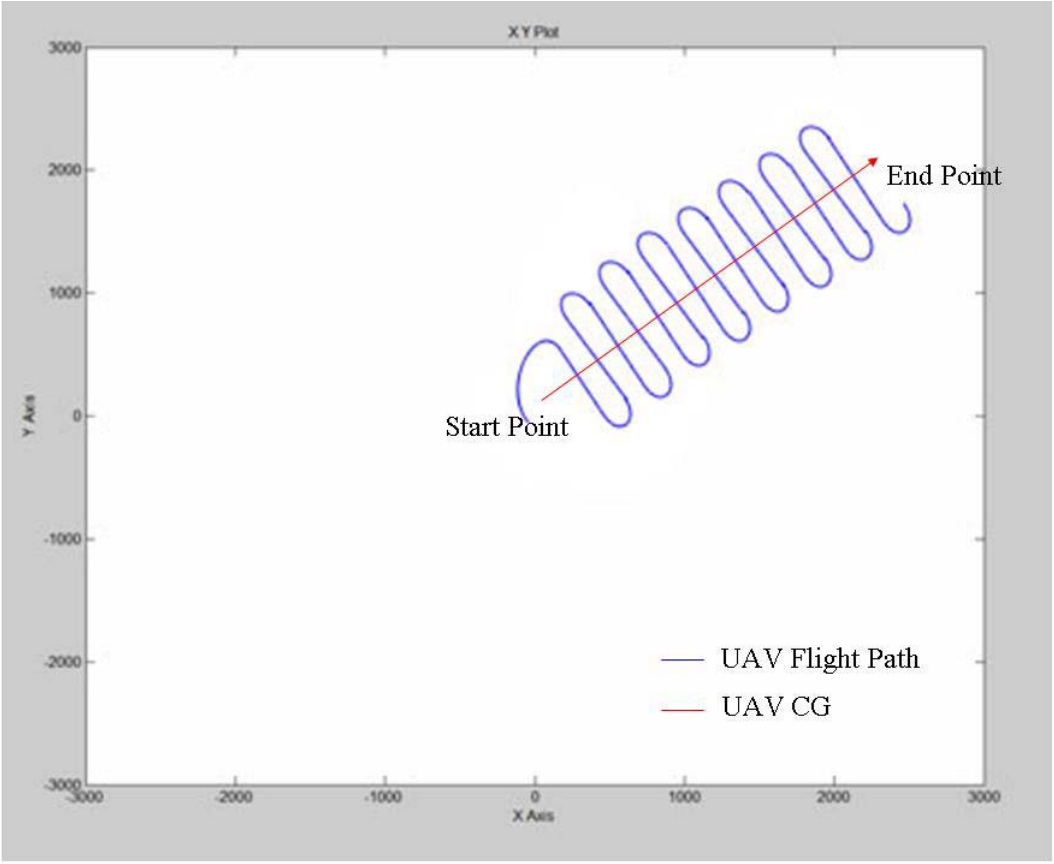

Figure 15. "S" Curve Flight Path

The camera gimbal controller uses the state condition of the UAV from the UAV six-DOF model and the fixed position forward of the AGV to determine the pan and tilt angle for the camera. The pan and tilt angle is sent to the camera keystone model to derive the positions that the field of view of the camera projects onto the ground.

The model uses the GeoTiff map of the Camp Roberts, CA area (in the vicinity of 35.7N, 120.7E), for visualizing the simulation. The location of the UAV, the AGV, the fixed position forward of the AGV and the UAV CG are superimposed over the GeoTiff map to provide a sense of location. The keystone effect is shown on the GeoTiff map. The model uses relative position for all computations and is subsequently translated into the GeoTiff map coordinates using a conversion factor for the location as follows:

Latitude conversion factor = 111119.99966 m/degree

Longitude conversion factor = 91023.79479 m/degree

The conversion factors are applied to the x-coordinate and y-coordinate only. The z-coordinate is unaffected due to the flat earth assumption that the model is using.

THIS PAGE INTENTIONALLY LEFT BLANK

III. SIMULATION AND RESULT

The output of the simulation shows that the UAV is able to accurately point the camera at the fixed forward position of the AGV along the road while following the flight path generated by the flight path control algorithm. The outputs are shown in the following figures.

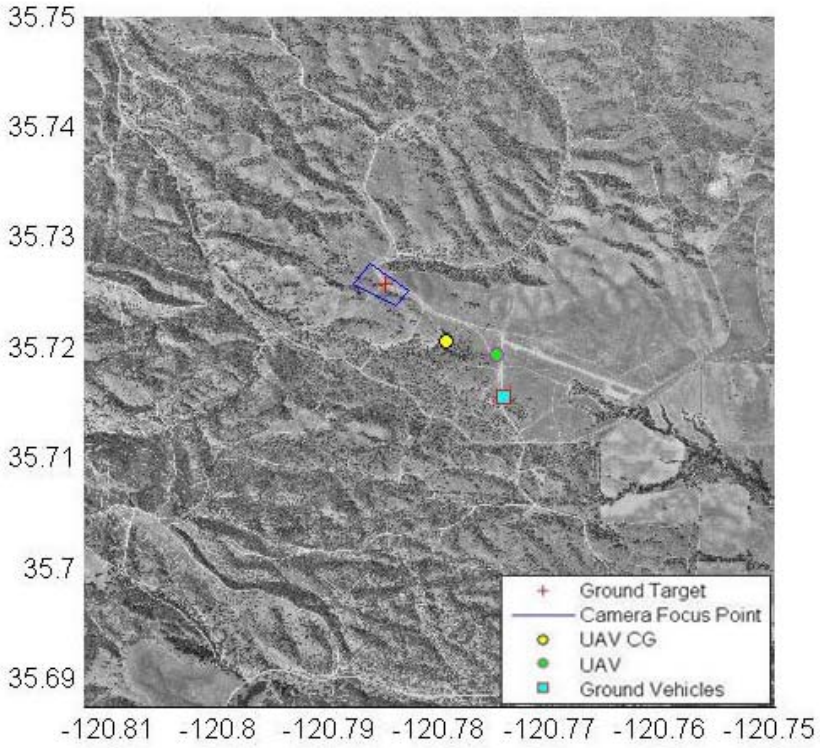

Figure 16. Output of Simulation 1

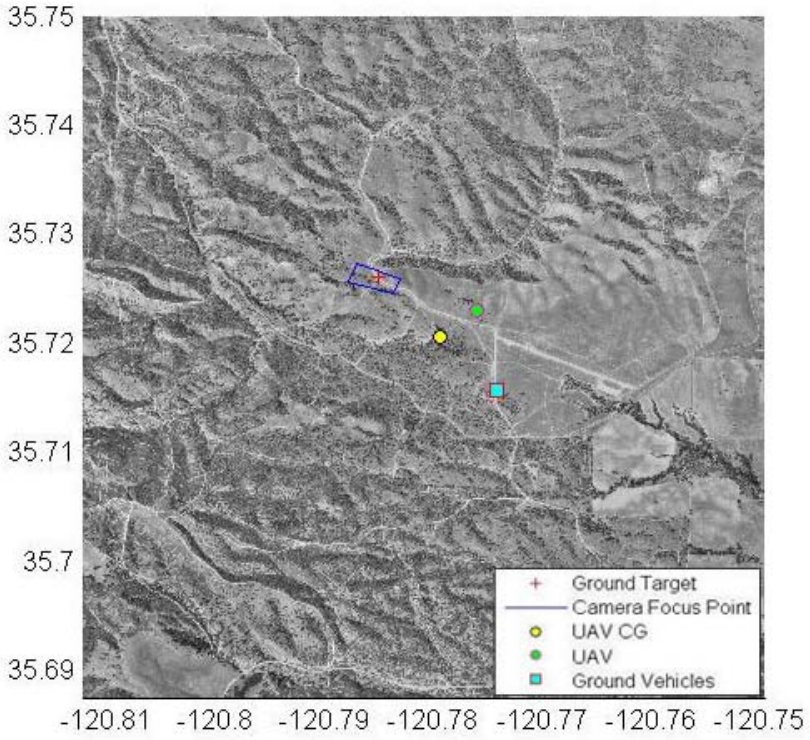

Figure 17. Output of Simulation 2

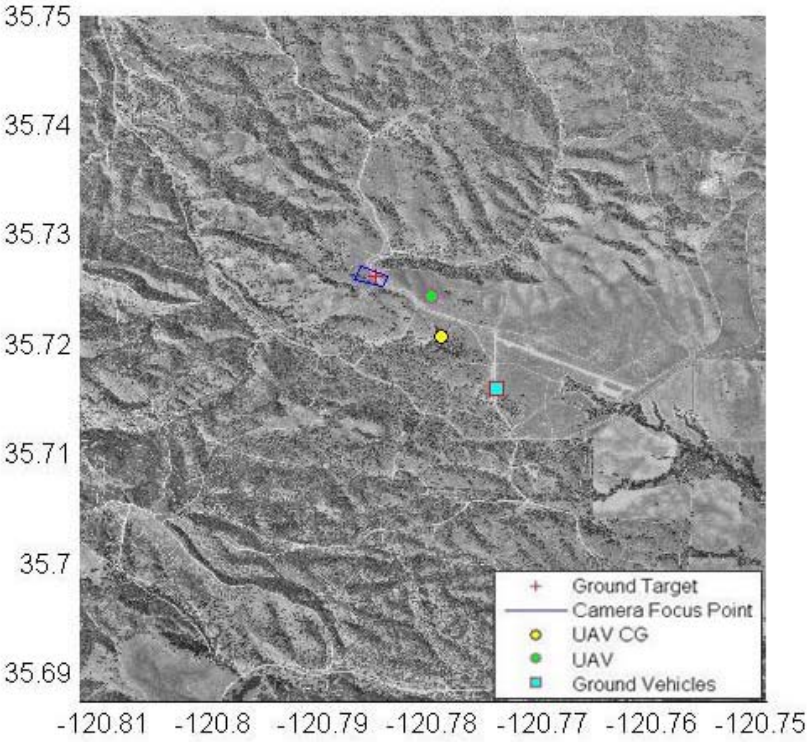

Figure 18. Output of Simulation 3

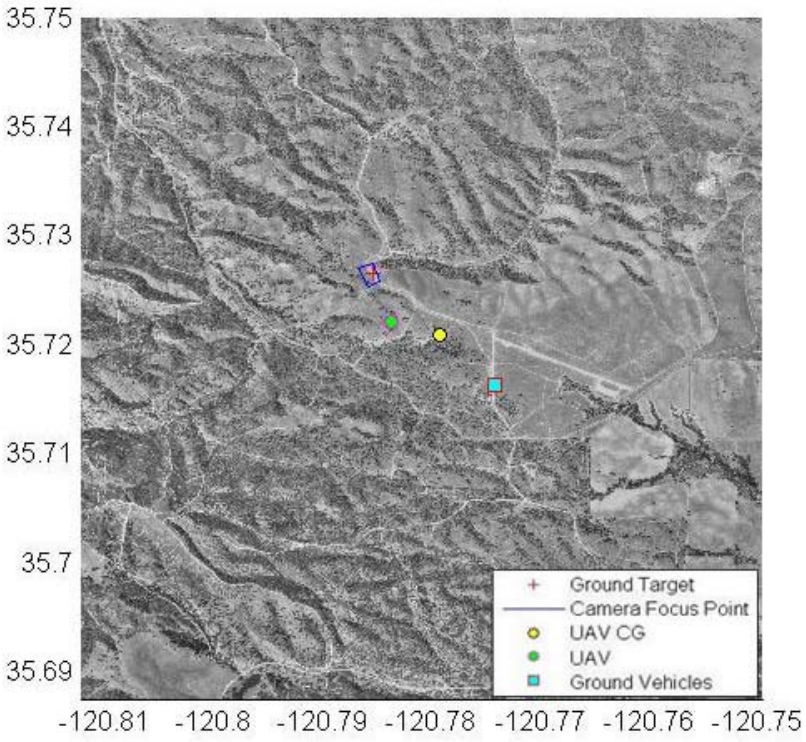

Figure 19. Output of Simulation 4

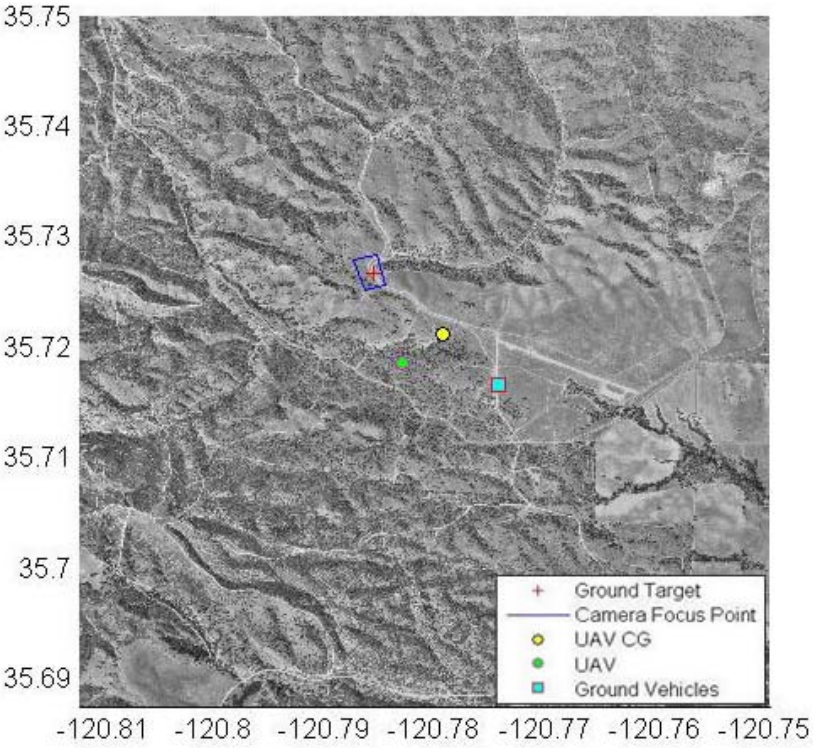

Figure 20. Output of Simulation 5

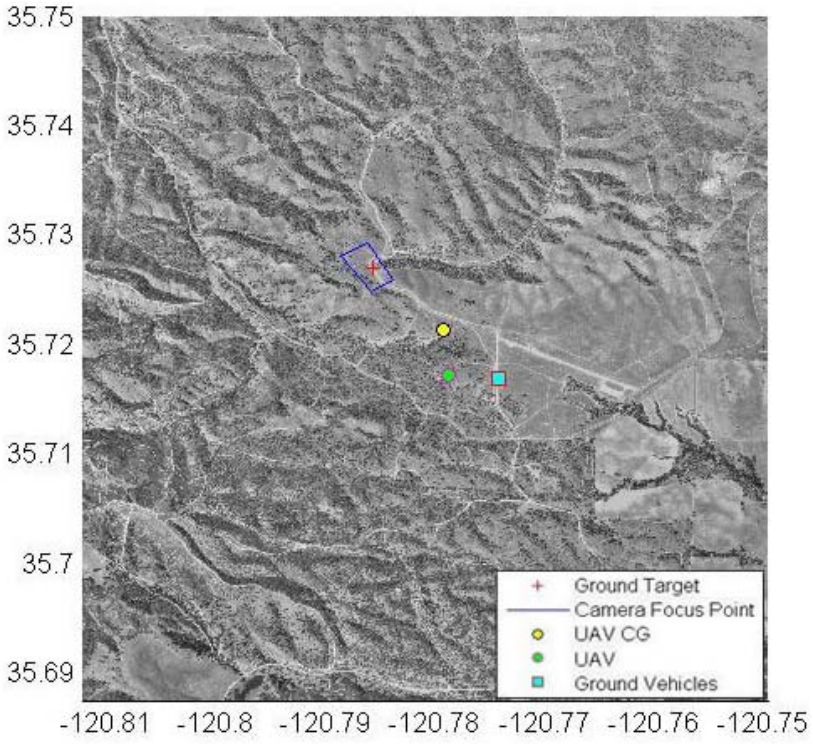

Figure 21. Output of Simulation 6

From the figures above, it can be seen that the UAV is flying in a circular path around the UAV CG with a relative constant desired horizontal range. The AGV and the fixed position forward of the AGV are moving along the road shown in the GeoTiff Map. The area in which the image is captured by the onboard camera shows that the camera is able to track the fixed forward position effectively. The keystone effect is also shown.

This simulation shows that the area captured by the camera image is constantly changing due to the position of the UAV. The area captured is bigger when the UAV is flying further away from the fixed forward position. This is undesirable and further work should be done to provide an active zoom control to create a constant area captured by the camera that is independent from the UAV position.

The camera is out of focus from the fixed position forward of the AGV at the start of the simulation. This is due to the time lag of the camera pan and tilt mechanisms that are incorporated into the model. The initial pan and tilt angle of the camera is set at zero degrees, which requires the camera gimbal control algorithm to correct the camera pan and tilt angle in order to track the ground target. This is shown in Figure 24.

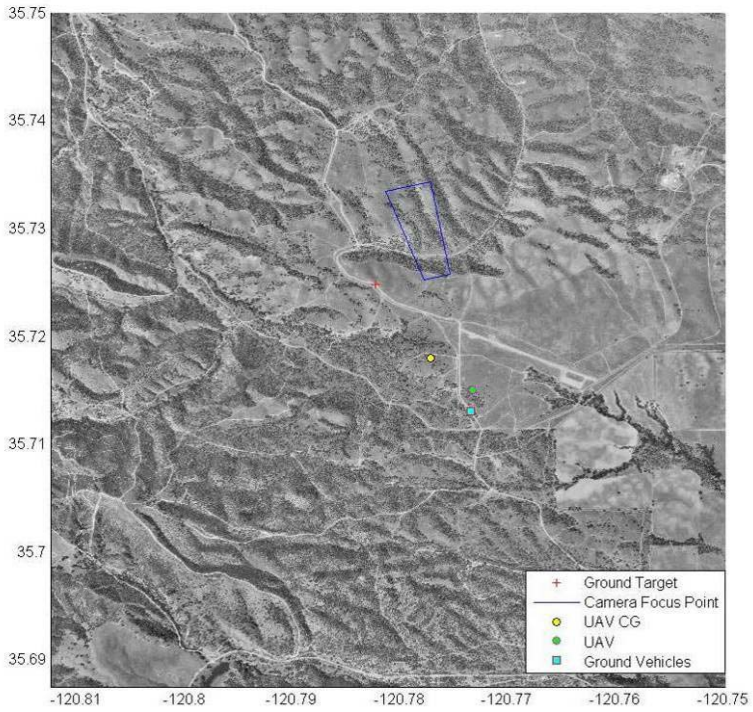

Figure 22. Camera Start-up Error

The initial speed and heading of the UAV plays an important part for the UAV flight control algorithm. From Figure 23, it can be seen that the UAV is further from the UAV CG location. The relative position of the UAV and the UAV CG is larger than the desired horizontal range determined by the tether control algorithm. This is due to the start location of the UAV, which is set at 35.71N, 120.77E and the initial heading of the UAV is set to due east. It can also be seen that the UAV is correcting its path toward the UAV CG by changing its heading gradually to north. This gradual movement is due to the minimum turning radius that is related to the flight characteristic of the UAV.

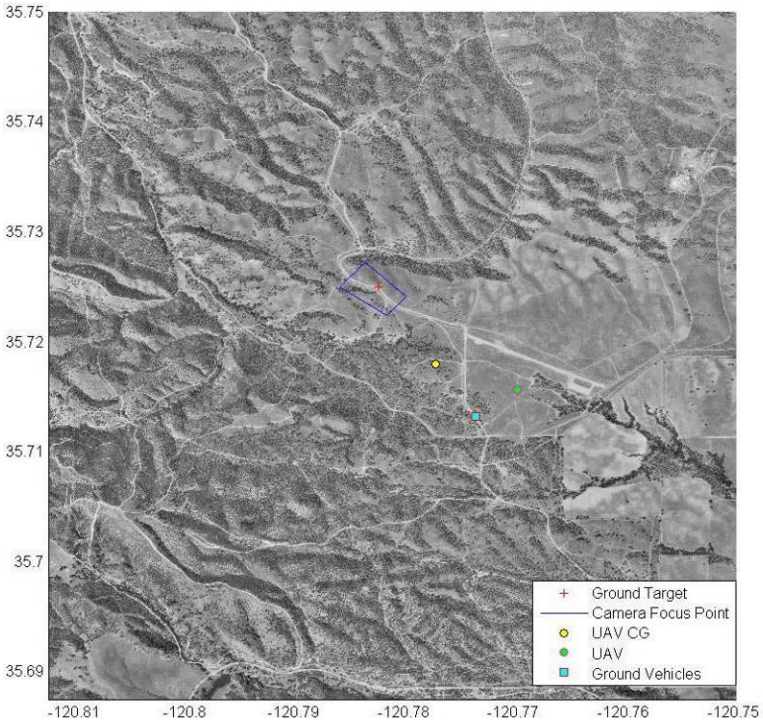

Figure 23. UAV Initial Flight Correction

From the simulation output above, it is noted that the location of the UAV CG does not follow a road. This is due to the fact that the UAV CG is an imaginary target location for the UAV flight control algorithm to take as a reference for planning the flight path of the UAV. The UAV CG location is determined by the tether control algorithm, given the signal strength of the communication between the UAV and the AGV. The location of the UAV CG is strategically positioned to be between the target location and the AGV to achieve the optimum effect of creating a flight path that is near the target and within communication range.

IV. CONCLUSION AND RECOMMENDATION

The ability to integrate a heterogeneous mix of unmanned vehicles has great potential in enhancing military operations and provides better real-time situation awareness of the battlefield. With the advancements in unmanned vehicles including high speed real-time obstacle avoidance and intelligent path planning and correction, there is a need to research the integration of various unmanned platforms to achieve a single mission.

This thesis looks into the three problems associated with the integration of the UAV and the AGV: the development of an autopilot guidance strategy to compensate for the relative speed differences between the UAV and the AGV, the keystone effect of the image from projecting the camera's field of view onto the ground given the pan and tilt from the onboard camera of the UAV, and the need to ensure the reliability of the communication network between the UAV and the AGV with the limited range of the communication equipment.

The results show that these problems associated with the integration of the UAV and the AGV can be overcome. The first problem, the relative speed difference between the UAV and the AGV, was overcome by using a circular flight path for the UAV to compensate for the slower speed AGV. The second problem, associated with the distortion of the captured image due to the keystone effect of the camera, was addressed by a model to identify the actual area captured by the image. The third problem, which arose from the need to provide reliable communication between the UAV and the AGV with the limited communication range of the equipment, was overcome by implementing a tether control between the UAV and the AGV.

From the result of this thesis, where the UAV is able to integrate with the AGV, this concept could be used for the UAV to integrate with an Unmanned Surface Vehicle (USV) to provide forward reconnaissance for the USV when traveling along a river.

From this research, it is recommended that a target search model be incorporated to allow the UAV to conduct a search along a series of routes that lead to the advancement of the AGV. This will provide preemptive warnings to the AGV on

possible obstacles to be encountered, for example, a vehicle traveling toward the planned route of the AGV that might cause the obstruction of the AGV. The search model could take reference from the Rapidly-exploring Random Trees (RRT)-Connect proposed by James J. Kuffner in [15]. The RRT is a simple and efficient randomized algorithm for solving single-query path planning problems in high-dimensional configuration spaces. The RRT-Connect provides an effective way to conduct path planning and identify an alternative route, where such a route could pose as an avenue for other vehicles that could travel into the planned path of the AGV and disrupt the operation.

A dynamic road demarcating algorithm is recommended to replace the sets of discreet coordinates representing the road in the current model. The simulation used a set of discreet predetermined coordinates to identify the road network on the GeoTiff Map. The nature of military operations frequently entails the creation and destruction of roads, thus incorporating a dynamic road demarcating algorithm would be attractive to any military operation.

It is also recommended that an active zoom control for the camera be incorporated into the camera control model to enhance the stability of the captured video by maintaining a relatively constant area of view from the camera.

While this thesis looked into using the UAV to provide forward reconnaissance for the AGV, the roles can be reversed. The AGV or USV could provide close-in surveillance on positions of interest that are determined by the UAV. Such an application is useful in a scenario where the UAV has identified a position or object of interest and requires further investigation or physical presence on the position or object. In locations where the position of the tracked target is occluded, the AGV can maintain position lock until the UAV can continue its tracking.

Finally, the UAV can be used for effective, real-time path planning for the AGV in built-up areas. The UAV, with its unobstructed flight path at high altitude, could provide real-time information for the AGV path planning. This would effectively reduce the possibility of detection of the AGV by the enemy, and thus improve survivability. One problem that is associated with UAV operation in built-up areas, is the high

probability of losing the autonomous tracking of the target, thus further research is necessary to explore the effects of such occlusion and methods need to be devised to overcome this problem.

In conclusion, the work done in this thesis has shown the possibility and the potential of integrating heterogeneous unmanned vehicles. The collaborative nature of integrating the unmanned vehicles would inevitably enhance the effectiveness of the vehicles in a wide variety of applications.

THIS PAGE INTENTIONALLY LEFT BLANK

APPENDIX A. CAMERA GIMBAL CONTROL MODEL

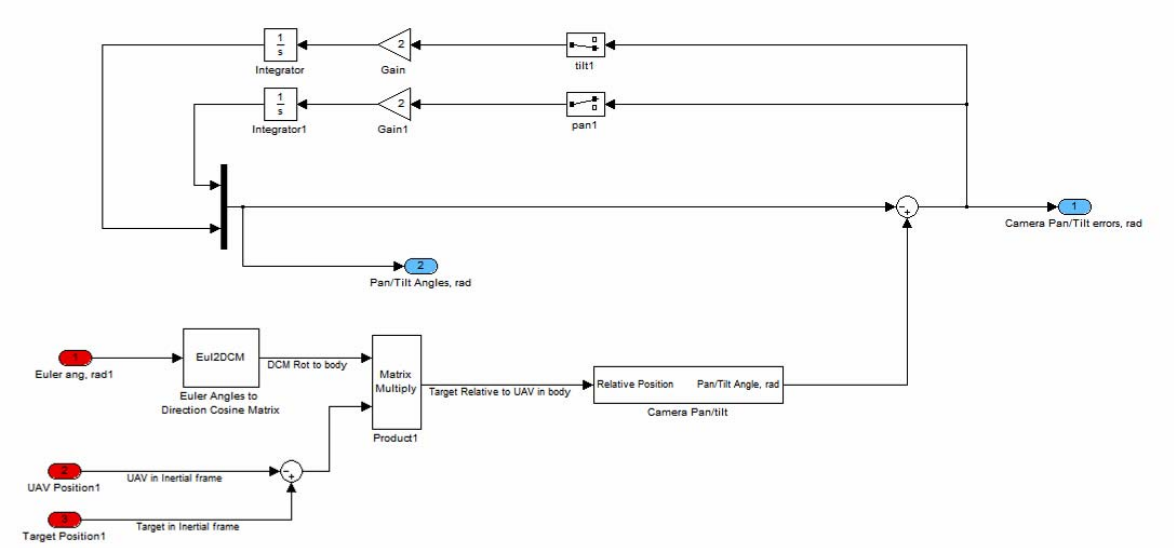

A. CAMERA PAN/TILT MODEL

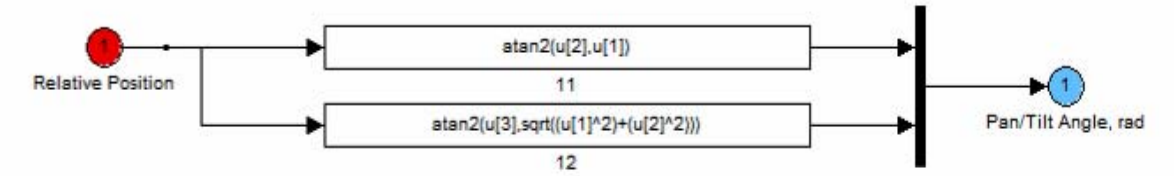

THIS PAGE INTENTIONALLY LEFT BLANK

APPENDIX B. CAMERA KEYSTONE MODEL

A. CAMERA MODEL

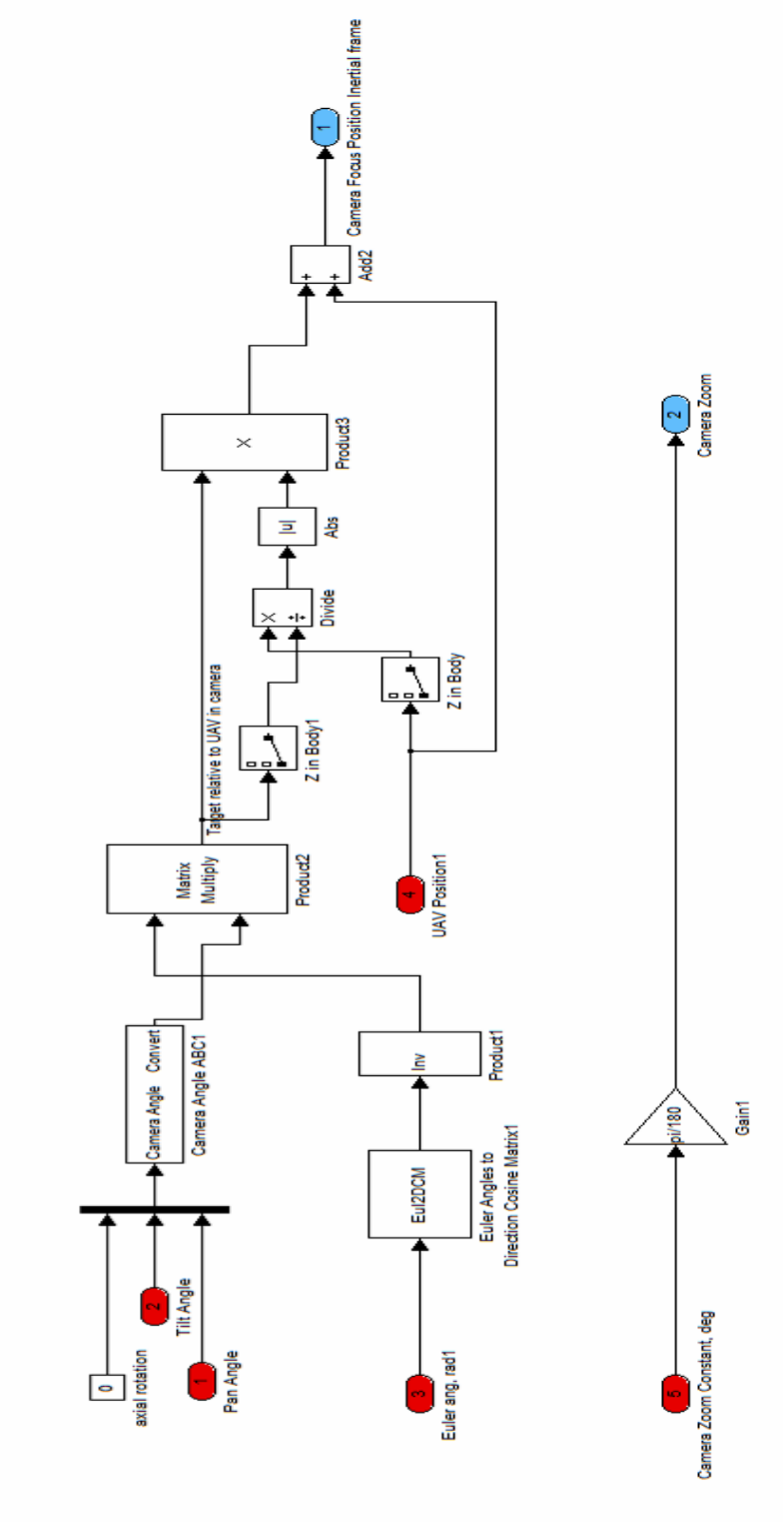

B. CAMERA ANGLE ABC1

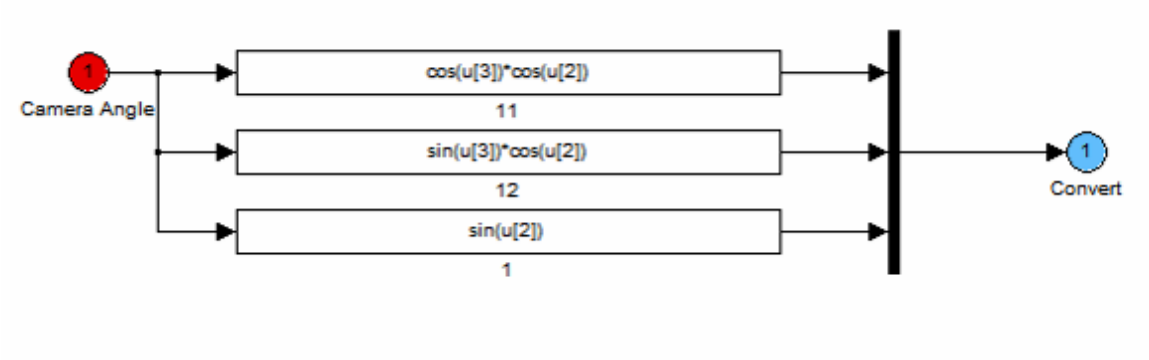

C "TGTTRACKING.M" LISTING

```
function [sys,x0,str,ts] = sldemo_tanksfun(t,x,u,flag)

switch flag,

% Initialization %
case 0,
[sys,x0,str,ts]=mdlInitializeSizes;

% Update %
case 2,
sys=mdlUpdate(t,x,u);

% Unhandled flags %
case { 1, 3, 4, 9 }
sys=[];

end
% end sldemo_tanksfun

%=============================================================================
% Return the sizes, initial conditions, and sample times for the S-function.
%=============================================================================
function [sys,x0,str,ts]=mdlInitializeSizes
sizes = simsizes;
sizes.NumContStates  = 0;
sizes.NumDiscStates  = 0;
sizes.NumOutputs     = 0;
sizes.NumInputs      = 18;
sizes.DirFeedthrough = 1;
sizes.NumSampleTimes = 1;

sys = simsizes(sizes);


% initialize the initial conditions
x0  = [];
str = [];              % str is always an empty matrix

% initialize the display figure
```

```
ts  = [0 0];
figure (1)
mapshow('35120f72.tif');
hold on;
xlim=[-120.79 -120.75];
ylim=[35.70 35.73];
% end mdlInitializeSizes


%=============================================================================
% Handle discrete state updates, sample time hits, and major time step requirements.
%=============================================================================
function sys=mdlUpdate(t,x,u) %#ok

% initialize the return arg
sys=[];
TgtX=u(1);
TgtY=u(2);
TgtZ=u(3);
CamX=u(4);
CamY=u(5);
CamZ=u(6);
CGX=u(7);
CGY=u(8);
CGZ=u(9);
UAVX=u(10);
UAVY=u(11);
UAVZ=u(12);
CamZm=u(13);
Pan=u(14);
Tilt=u(15);
GVX=u(16);
GVY=u(17);
GVZ=u(18);

D=sqrt((CamX-UAVX)^2+(CamY-UAVY)^2+(CamZ-UAVZ)^2);
D1=D*sin(Tilt)/sin(pi-CamZm-Tilt);
D2=D*sin(pi-Tilt)/sin(Tilt-CamZm);
U1=D*sin(CamZm)/sin(pi-CamZm-Tilt);
U2=D*sin(CamZm)/sin(Tilt-CamZm);
R=D*tan(CamZm);
R1=D1*tan(CamZm);
R2=D2*tan(CamZm);
Pan=atan2((CamY-UAVY),(CamX-UAVX));
Tilt = atan2(sqrt(((CamY-UAVY)^2)+((CamX-UAVX)^2)),(CamZ-UAVZ));

Lat0=35.7114;                                   %Y Datum
Lon0=-120.77256;                                %X Datum
LatCov=111119.99965975754;                      %m/deg for Latitude
LonCov=91023.7947885214;                        %m/deg for Longtitude

Focx(1)=((CamX-U1*cos(Pan))+(R1*sin(Pan)));
Focx(2)=((CamX+U2*cos(Pan))+(R2*sin(Pan)));
Focx(3)=((CamX+U2*cos(Pan))-(R2*sin(Pan)));
Focx(4)=((CamX-U1*cos(Pan))-(R1*sin(Pan)));
```

```
Focx(5)=((CamX-U1*cos(Pan))+(R1*sin(Pan)));

Focy(1)=((CamY-U1*sin(Pan))-(R1*cos(Pan)));
Focy(2)=((CamY+U2*sin(Pan))-(R2*cos(Pan)));
Focy(3)=((CamY+U2*sin(Pan))+(R2*cos(Pan)));
Focy(4)=((CamY-U1*sin(Pan))+(R1*cos(Pan)));
Focy(5)=((CamY-U1*sin(Pan))-(R1*cos(Pan)));

FocLon=Lon0+Focx/LonCov;
FocLat=Lat0+Focy/LatCov;

CGLon=Lon0+CGX/LonCov;
CGLat=Lat0+CGY/LatCov;

UAVLon=Lon0+UAVX/LonCov;
UAVLat=Lat0+UAVY/LatCov;

TgtLon=Lon0+TgtX/LonCov;
TgtLat=Lat0+TgtY/LatCov;

GVLon=Lon0+GVX/LonCov;
GVLat=Lat0+GVY/LatCov;

hold on
h=findobj('Color','r');
delete(h);
h=findobj('Color','b');
delete(h);
h=findobj('Color','m');
delete(h);
h=findobj('Color','y');
delete(h);
h=findobj('Color','k');
delete(h);
h=findobj('Color','c');
delete(h);

plot(TgtLon,TgtLat,'+r');
plot(FocLon,FocLat,'b');
plot(CGLon, CGLat,'ok', 'MarkerFaceColor','y');
plot(UAVLon, UAVLat,'om','MarkerFaceColor','g');
plot(GVLon, GVLat,'sr','MarkerFaceColor','c')
h = legend('Ground Target','Camera Focus Point','UAV CG','UAV','Ground Vehicles',3);
legend('Ground Target','Camera Focus Point','UAV CG','UAV','Ground Vehicles',4);
```

APPENDIX C. TETHER CONTROL MODEL

A. TETHER CONTROL MODEL

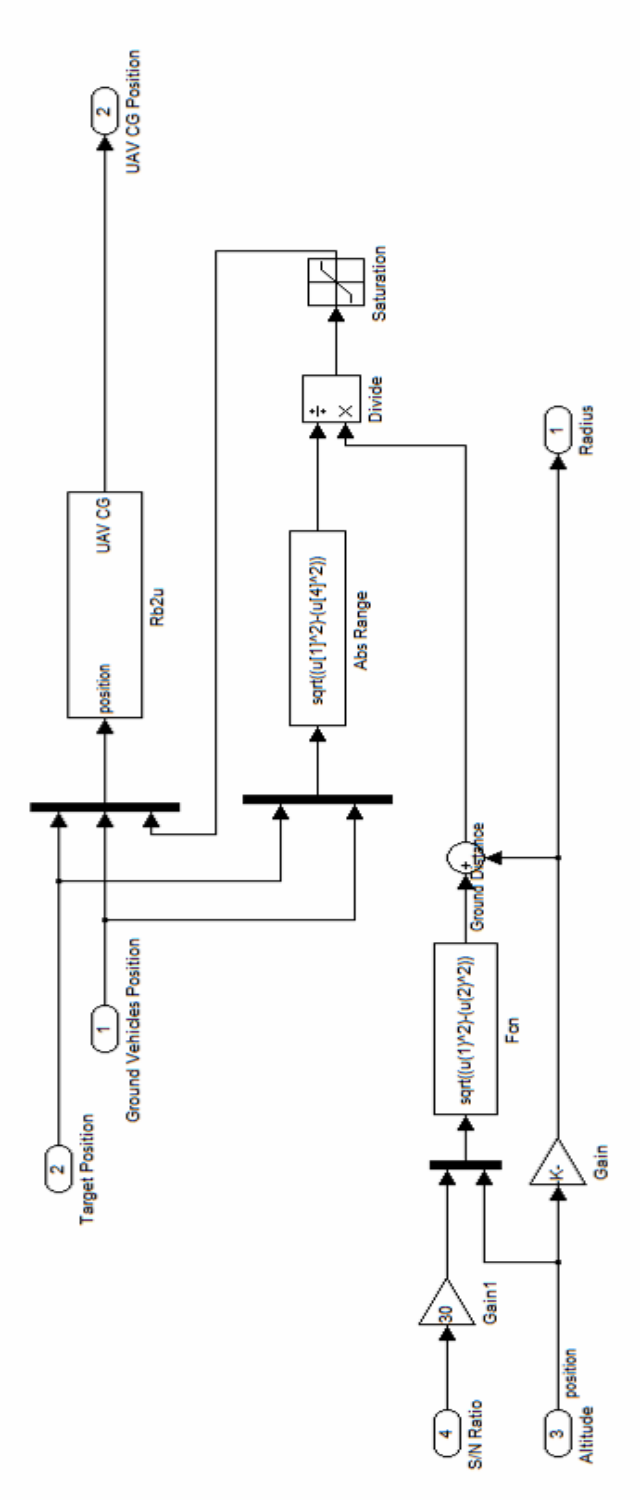

B. GROUND VEHICLES MODEL

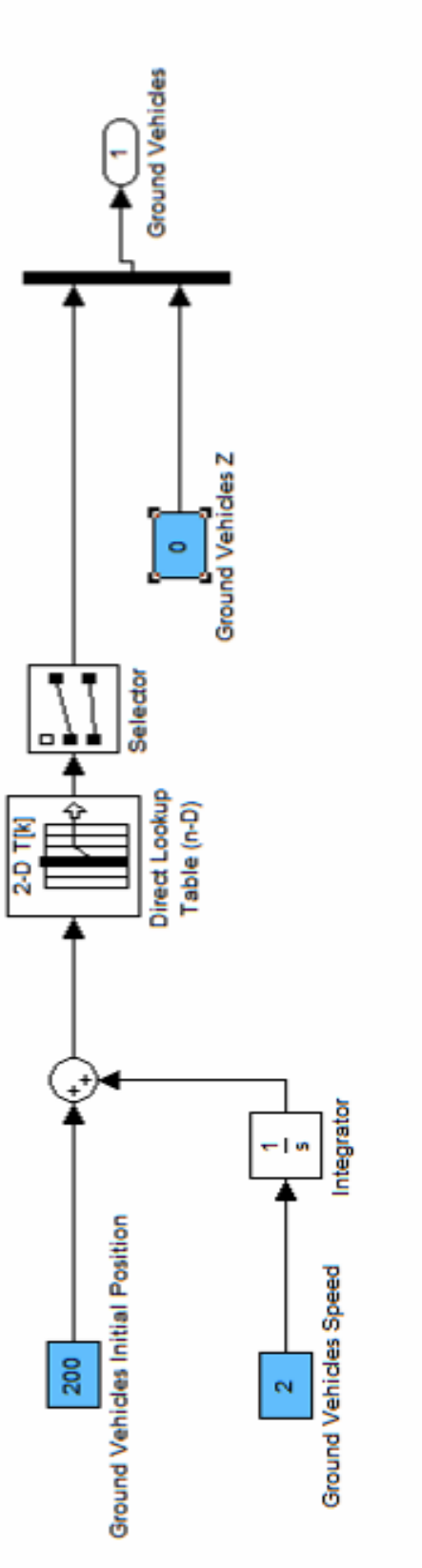

C. TARGET MODEL

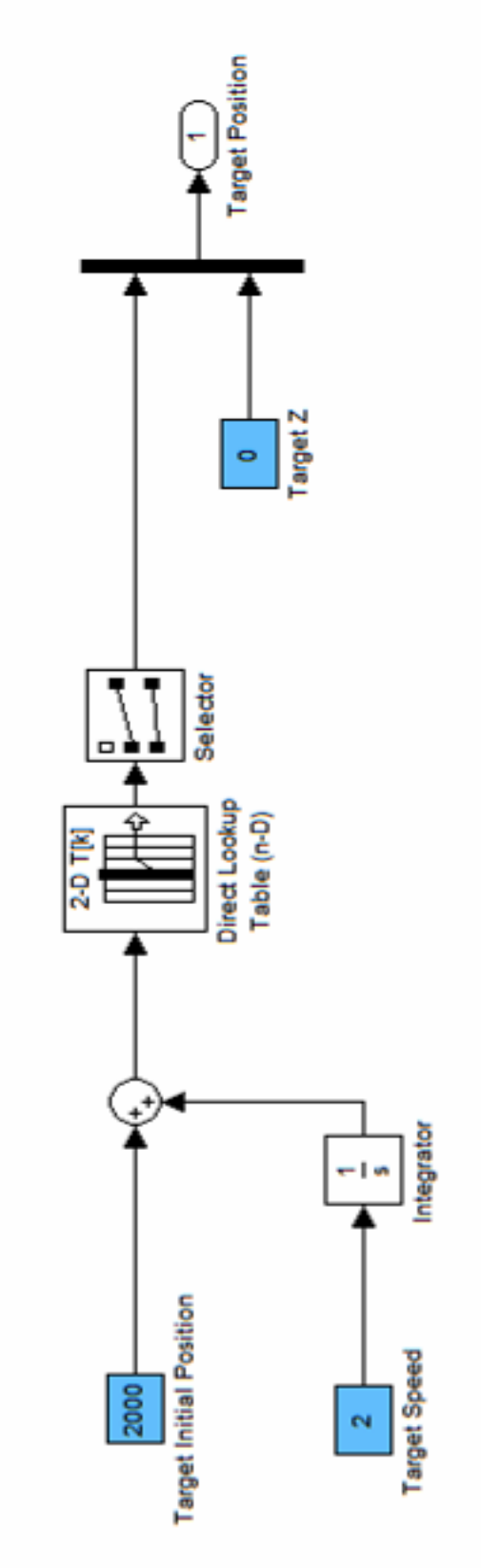

THIS PAGE INTENTIONALLY LEFT BLANK

LIST OF REFERENCES

1. Micromouse Competition Website: http://micromouse.cannock.ac.uk/index.htm. December 2006.

2. Seydou SOUMARE, Akihisa OHYA and Shin'ichi YUTA, "Real-Time Obstacle Avoidance by an Autonomous Mobile Robot using an Active Vision Sensor and a Vertically Emitted Laser Slit," The 7th International Conference on Intelligent Autonomous Systems (IAS-7), California, March 25–27, 2002.

3. Juan Carlos Rosete Fonseca, Efrén Gorrostieta Hurtado, Joaquin Perez Meneses, "Obstacles Avoidance in a Self Path Planning of a Polar Robot," CERMA, pp. 157–162, Electronics, Robotics and Automotive Mechanics Conference (CERMA '06), 2006.

4. Matthew Spenko, Karl Iagnemma, Steven Dubowsky, "High Speed Hazard Avoidance for Mobile Robots in Rough Terrain," Published in Gerhart, Grant R.; Shoemaker, Chuck M.; Gage, Douglas W., eds. Unmanned Ground Vehicle Technology VI. Proceedings of the SPIE, Volume 5422, pp. 439–450 (2004).

5. Stephen Griffiths, Jeff Saunders, Andrew Curtis, Tim McLain and Randy Beard "Obstacle and Terrain Avoidance for Miniature Aerial Vehicles," In Review, IEEE Robotics and Automation Magazine (2006).

6. Yvan Petillot, Ioseba Tena Ruiz, and David M. Lane, "Underwater Vehicle Obstacle Avoidance and Path Planning Using a Multi-Beam Forward Looking Sonar," IEEE J. Oceanic Eng., vol. 26, pp. 240–251, April 2001.

7. Douglas P. Horner, Anthony J. Healey, Sean. P. Kragelund, "AUV Experiments in Obstacle Avoidance," Proceedings of IEEE Oceans 2005 Conference.

8. Vladimir N. Dobrokhodov, Isaac I. Kaminer, Kevin D. Jones and Reza Ghabcheloo, "Vision-Based Tracking and Motion Estimation for Moving targets using Small UAVs," Proceedings of American Control Conference, Minneapolis, June 2006.

9. Douglas P. Horner, Anthony J. Healey, "Use of Artificial Potential Fields for UAV Guidance and Optimization of WLAN Communications," Proceedings of the IEEE AUV2004 Conference, Maine, June 2004.

10. Andrew Woods, Tom Docherty and Rolf Koch, "Stereoscopic Displays and Applications IV," *Proceedings of the SPIE Volume 1915*, San Jose, CA, Feb. 1993.

11. Eva Pärt-Enander, Anders Sjöberg, Bo Melin, and Pernilla Isaksson, "The MATLAB Handbook,"Addison-Wesley, 1998.

12. Sk. Sazid Mahammad and R. Ramakrishnan, “GeoTiff - A Standard Image File Format for GIS Applications,” Space Application Centre, ISRO, Ahemedabad.

13. Dr. Niles Ritter and Mike Ruth, “GeoTiff Format Specification - GeoTiff Revision 1.0,” SPOT Image Corp., (2000).

14. Brian L. Stevens and Frank L. Lewis, “Aircraft Control and Simulation,” 2nd edition, Wiley, pp. 59–142, 2003.

15. James J. Kuffner, Jr. and Steven M. LaValle, “RRT-Connect: An Efficient Approach to Single-Query Path Planning,” Proceeding of 2000 IEEE International Conference on Robotics and Automation, vol. 2, pp. 995–1001, 2000.

INITIAL DISTRIBUTION LIST

1. Defense Technical Information Center
   Ft. Belvoir, Virginia

2. Dudley Knox Library
   Naval Postgraduate School
   Monterey, California

3. Prof. Anthony J. Healey
   Department of Mechanical and Astronautical Engineering
   Naval Postgraduate School
   Monterey, California

4. Prof. Douglas Horner
   Department of Mechanical and Astronautical Engineering
   Naval Postgraduate School
   Monterey, California

5. Prof. Vladimir Dobrokhodov
   Department of Mechanical and Astronautical Engineering
   Naval Postgraduate School
   Monterey, California

6. Prof. Yeo Tat Soon
   Director of Temasek Defence Systems Institute (TDSI)
   Vice-Dean, Faculty of Engineering, Admin
   National University of Singapore
   Singapore

7. Tan Lai Poh
   Senior Admin Officer (MDTS)
   Temasek Defence Systems Institute (TDSI)
   National University of Singapore
   Singapore